AD 273 686

AFCRL-62-78

AN EXPERIMENTAL INVESTIGATION OF LUNAR AND AURORAL SCATTERED SIGNALS

PART I LUNAR ECHOES

Prepared for:

Electronics Research Directorate
Air Force Cambridge Research Laboratories
Office of Aerospace Research
United States Air Force
Bedford, Massachusetts

FINAL REPORT
By: H. A. Von Biel
Contract No. AF 19(604)-6116
Project No. 4603
Task No. 460308
CAL Report No. CM-1393-P-7
15 January 1962

CORNELL AERONAUTICAL LABORATORY, INC.
OF CORNELL UNIVERSITY, BUFFALO 21, N. Y.

"Requests for additional copies by Agencies of the Department of Defense, their contractors, and other Government agencies should be directed to the:

ARMED SERVICES TECHNICAL INFORMATION AGENCY
ARLINGTON HALL STATION
ARLINGTON 12, VIRGINIA

Department of Defense contractors must be established for ASTIA services or have their "need-to-know" certified by the cognizant military agency of their project or contract."

U. S. DEPARTMENT OF COMMERCE
OFFICE OF TECHNICAL SERVICES
WASHINGTON 25, D C

AFCRL-62-78

CORNELL AERONAUTICAL LABORATORY, INC.
BUFFALO, NEW YORK

CAL REPORT NO. CM-1393-P-7
CONTRACT NO. AF 19(604)-6116
PROJECT NO. 4603
TASK NO. 460308

FINAL REPORT

AN EXPERIMENTAL INVESTIGATION OF LUNAR AND AURORAL SCATTERED SIGNALS PART I LUNAR ECHOES

15 JANUARY 1962

BY H.G. von Biel
H. A. Von Biel
Project Engineer

APPROVED W. Flood
W. A. Flood, Head,
Radio Physics Section

APPROVED James W. Ford
James W. Ford, Head,
Applied Physics Department

PREPARED FOR:
ELECTRONICS RESEARCH DIRECTORATE
AIR FORCE CAMBRIDGE RESEARCH LABORATORIES
OFFICE OF AEROSPACE RESEARCH
UNITED STATES AIR FORCE
BEDFORD, MASSACHUSETTS

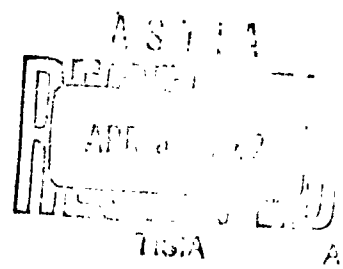

ABSTRACT

This report summarizes the work carried out, and the results obtained, in an experimental investigation of lunar echoes at 915 mc.

The transmission loss between isotropic radiators over the earth-moon-earth path was established as being 280 db at 915 mc. This result, in conjunction with transmission losses reported by other investigators in the frequency range from 200 mc to 3000 mc, leads one to the conclusion that the radar cross section of the moon is frequency dependent and decreases with increasing frequency at a rate of about 6 db per octave. At 915 mc, the lunar radar cross section was found to be equal to 4.2×10^{10} square meters.

After detection, the lunar echo at 915 mc exhibits Rayleigh-like fading with an average 10- to 90-percent fading range of about 14 db. There is evidence, however, that the lunar echo is not entirely randomly phased but contains a steady-signal component which is in the ratio of 1.5 to 1 with the rms scattered-signal components, i. e. 47 percent scattered power and 53 percent specular reflected power.

At 915 mc the lunar echo exhibited polarization changes between moonrise and moonset as large as 50 degrees; variations in excess of 30 degrees in the signal polarization have been measured on a day-to-day basis.

TABLE OF CONTENTS

Page

ABSTRACT iii

LIST OF ILLUSTRATIONS vi

I. INTRODUCTION 1

II. THEORETICAL DISCUSSION 3

III. EXPERIMENTAL PROCEDURE AND RESULTS 5

1. Transmission Loss and Amplitude Distributions . . . 6

2. Transmission Loss and Lunar Surface Scattering Properties 12

3. Faraday Rotation 27

IV. SUMMARY 33

APPENDIX A - EQUIPMENT 35

APPENDIX B - BEAM-TYPE PARAMETRIC AMPLIFIER 53

APPENDIX C - CALIBRATION OF 28-FOOT ANTENNA SYSTEM WITH NOISE SOURCES 55

A. Theory 55

B. Experimental Procedure 56

APPENDIX D - COMPUTATION OF MOON DOPPLER MAP 63

1. Introduction 63

2. The Doppler Effect 63

3. Positions and Velocities on the Earth and Moon 64

A. On the Earth 64

B. Matrix Representation 65

C. On the Moon 67

D. Velocity of the Point on the Moon . . 71

4. The Angles of Propagation 71

5. Plan of Calculation 74

LIST OF ILLUSTRATIONS

Figure		Page
1	Lunar Doppler Shift at 915 Mc/S	7
2	Average of Eleven 5-Minute Amplitude Distributions	9
3	Cumulative Distribution of Lunar Echo	10
4	Lunar Echo - Signal-to-Noise Ratio and Transmission Loss Measured over One Lunar Cycle Path: Bedford-Moon-Newstead	13
5	Lunar Echo Signal-to-Noise Ratio and Transmission Loss Plotted as a Function of Probability of Occurrence	14
6	Typical Lunar Echo Spectra	16
7	Example of Computed Contours of Constant Doppler Shift Plotted in Lunar Coordinates	17
8	Constant Doppler Frequency Contour Separation as a Function of Time	18
9	Angular Spectrum of Lunar Echo	20
10	Relative Power as a Function of Time Delay and Lunar Range Depth	21
11	Relative Power as a Function of Lunar Surface Area	22
12	Relative Power as a Function of Lunar Surface Area (Logarithmic Plot)	23
13	Percent Total Energy as a Function of Lunar Surface Area	24
14	Lunar Circuit Transmission Loss between Isotropic Radiator and Collector as a Function of Frequency	26
15	Diurnal Variation of the Lunar Echo Polarization, 8 - 9 June 1960	29
16	Diurnal Variation of the Lunar Polarization, 9 - 10 June 1960	30
17	Diurnal Variation of the Lunar Echo Polarization, 10 - 11 June 1960	31
18	Lunar Echo Relative Polarization vs Declination at Meridian Transit (Newstead)	32
19	Lunar and Auroral Echo Receiver, Block Diagram	
20	Receiver Console	36
21	Antenna, Feed Horn, and Parametric Amplifier	37
22	Recording Scheme for Lunar Echo at 200 cps I.F. and Data Reduction Technique, Block Diagram	41

LIST OF ILLUSTRATIONS (contd.)

Figure		Page
23	Radio Astronomy Recording Set-up	43
24	Digital Recording System	45
25	Experimental Set-up for Polarization Measurements . .	46
26	Sample Recording: Data Used to Determine Lunar Echo Polarization	47
27	915-Mc Receiver Characteristics: 4-7-61	50
28	100-Kc I. F. Detector Characteristic Relative Input Voltage at 915 Mc	51
29	915-Mc Receiver Characteristics: 4-7-61	57
30	Cygnus-A Drift Pattern (4-11-61 - 1030 EST)	59
31	Cassiopeia-A Drift Pattern (4-11-61 - 1805 EST) . .	60

I. INTRODUCTION

Since the U. S. Army Signal Corps announced the first successful radar contact with the moon in 1946, there has been increased interest in experimental investigations of lunar radio echoes.

After completing an experimental and theoretical investigation of tropospheric scatter propagation at 915 mc, the Cornell Aeronautical Laboratory,[1] in 1959, proposed an experimental lunar echo program that would use the tropospheric-scatter propagation transmitter and receiver available from that study. Because the 10-kilowatt c-w transmitter (located in Bedford, Massachusetts) and receiver (located at Newstead, New York) were physically separated by about 400 miles, c-w operation was planned for that particular earth-moon-earth circuit. In most of the lunar echo experiments performed in the past ten years, pulsed radio energy emissions were used. Because early theories predicted the moon to be rough at radio frequencies, it was expected that the returning radar pulse would be spread out in time to about 11.5 milliseconds. Even though there is evidence[2] that detectable amounts of radio energy can be found 11.5 milliseconds after the leading edge of the echo pulse, it soon became apparent that 90 percent of the total energy returned from the moon came from a small central area on the lunar surface. In addition to the unexpectedly small radar range depth observed, the lunar echoes faded periodically.

In 1951, Kerr and Shain[3] isolated the causes for the echo fading as being a combination of librational Doppler fading and periodic cross polarization of the echo caused by the Faraday effect in the ionosphere. In our lunar echo

---

[1] Tropospheric scatter propagation, Contract AF 19(604)-1835.

[2] Leadabrand, R. L., et al. Evidence that the Moon is a Rough Scatterer at Radio Frequencies, Stanford Research Institute Report 2-2604, February 1960, Contract AF 30(602)-1871.

[3] Kerr, F. J. and Shain, C. A., Moon Echoes and Transmission Through the Ionosphere, Proc. IRE, 37, 230-242 (1951).

experiment the phenomenon of librational Doppler fading was used to describe the scattering characteristics of the lunar surface, and even though the Faraday effect was expected to be negligibly small at 915 mc, an investigation of echo polarization changes was planned.

It is the purpose of this report to describe the lunar echo experiment performed and to summarize the results obtained.

II. THEORETICAL DISCUSSION

Lunar echo experiments performed during the past ten years have shown that a radio signal reflected by the moon fades sporadically. Slow and deep fading has been observed, particularly at VHF, in addition to rapid and apparently incoherent signal strength variations. It was soon discovered that the Faraday effect in the earth's ionosphere was responsible for the slow fading, and it was reasoned that the rapid fading was caused by the librational Doppler effect on the moon.

The Faraday effect causes the field vectors of a linearly polarized wave propagating through a magneto-ionic medium such as the earth's ionosphere to be rotated in a plane of constant phase. Thus, Faraday fading of the lunar echo is observed when a cross-polarized signal arrives at a linearly polarized receiving antenna. Because Faraday rotation is most severe at low frequencies (about 20 mc) and varies as λ^2, the frequency of fading caused by cross polarization is expected to be negligibly small at 915 mc.

Librational Doppler fading, on the other hand, is caused primarily by the rotation of the moon about its axis and is expected to be prominent at L-band frequencies. It is well known that the moon always presents the same face to the earth and that the moon completes one orbit around the earth roughly every 28 days. Consequently, the angular velocity of the moon is approximately 2π radians per 28 days, or about 2.6×10^{-6} radians per second. If it were assumed that the moon, instead of being a spheroid, were a circular plate, then the velocity relative to an observer on earth of any point on the diameter perpendicular to the spin axis would be determined by the product of the angular velocity and the distance of this point from the center. Thus, a point one lunar radius R (1740 km) from the center of this disc would either come toward or move away from the observer at a velocity of about 4.5 meters per second.

If a radio wave is reflected from a point at a distance r from the axis of rotation of this disc, it would suffer a Doppler shift, the reflected frequency being given by

$$f = f_o\left[1 \pm \frac{2r}{R}\left(\frac{+.5}{3}\right) \times 10^{-8}\right] \text{cps}$$

where R is the radius of the disc. Therefore, contours of constant frequency on the surface of the disc, would appear as straight lines parallel to the spin axis. If it is assumed that the area enclosed by adjacent lines of constant frequency and the circumference of the disc consists of a large number of individual scattering areas, the vector sum of all the individual echoes at a given frequency will have a certain phase. An instant of time later, if either the disc or the observer on earth has moved, the vector sum of these same echoes will be at a completely different phase. This argument will finally lead to the conclusion that the phase of the total echo at any given frequency is random, and that the total power per unit bandwidth received at any given frequency is the sum of all the powers per unit bandwidth scattered by the individual scattering areas. This, of course, implies that the amplitudes of the resulting echoes are Rayleigh distributed.

A similar argument can be used to predict the behavior of the moon (rather than a disc). Appendix D outlines a procedure by which contours of constant Doppler shift on the lunar surface may be calculated. If in addition to this calculation the frequency spectrum of the lunar echo can be obtained by some experimental technique, it is possible to deduce the angular spectrum of the individual scattering areas. Furthermore, on the assumption that the amplitude distribution is near Rayleigh for the lunar echo, the total power in the lunar echo is equal to the sum of the incremental powers returned from the individual scattering areas.

In the following sections of this report, the experimental procedures used and the results obtained will be discussed.

III. EXPERIMENTAL PROCEDURE AND RESULTS

The lunar echo experiment had four objectives:

(1) The determination of the earth-moon-earth circuit transmission loss at 915 mc

(2) An attempt to associate the amplitude distribution of the lunar echo with some process that is statistically describable

(3) The determination of the scattering properties of the lunar surface

(4) Observation of the Faraday effect on the polarization of the lunar echo.

In the following discussion there will be described three independent experiments from which the data required to accomplish these four objectives were obtained. Specifically, transmission loss and amplitude distribution data were obtained from the detected lunar echo, transmission loss and lunar surface scattering properties were deduced from the predetection frequency spectrum of the lunar echo, and the Faraday effect was observed by determining the polarization of the lunar echo. These topics are discussed at length in parts 1 - 3, respectively, of this section. The equipment used for the experiments is described in detail in Appendix A.

Whenever possible, all data required for the experiments were recorded simultaneously. Most of the data were collected on Mondays, Wednesdays, and Fridays from one hour before meridian transit at Newstead, New York, to one hour after meridian transit. It was possible to maintain this transmission schedule rigidly for $1\frac{1}{2}$ months. Ten moonrise to moonset transmissions, during which data were collected at half-hour intervals were conducted, and additional data were obtained sporadically throughout the performance period. Even though good agreement was found to exist between the data collected successively over the $1\frac{1}{2}$-month interval and those data collected on random days during the lunar cycle, the data obtained on consecutive days were used to construct most of the curves presented in this section.

Prior to each series of measurements, the receiving equipment was calibrated in frequency and polarization against the transmitter by using the tropospheric scatter-propagation mode between the receiver and transmitter site. The direct determination of the transmitted frequency and subsequent determinations of the moon bounce frequency permitted a measurement of the mean Doppler shift caused by the relative motion between earth and moon. While precise determination of the lunar echo frequency was not a required part of the program, a knowledge of mean Doppler shift provided a running check on the computed Doppler frequencies required to construct contours of constant Doppler shift on the lunar surface map. Figure 1 shows the computed theoretical mean Doppler frequencies and experimentally obtained frequencies, both plotted as a function of time. The plot shows fairly good agreement between the two frequencies in addition to substantiating an over-all equipment frequency stability of approximately one part in 10^8 per hour.

1. Transmission Loss and Amplitude Distributions

The recording equipment shown in Figure 24 (Appendix A) was used to collect video data of the lunar echo. Because the frequency counter used in the digital recording scheme was capable of only minimum hold- and display-times of 0.1 second each, the highest data rate obtainable from the apparatus was 5 samples per second. At that rate, 1500 independent samples of the lunar echo were collected in five minutes. The adequacy of 1500 data points for constructing meaningful amplitude distributions of the lunar echo was verified by comparing them with several 10-minute, 20-minute and 30-minute data runs. No significant difference in the resulting amplitude distributions was noticed.

As is shown in Figure 24, the detected lunar echo data were punched in standard teletype code on perforated tape and subsequently were permanently recorded on IBM cards. The Laboratory-owned IBM 704 computer was programmed to compute from these data the mean value, variance, and standard deviation. An additional step in the program normalized the raw data from "volts out" to units of standard deviation σ, and provided for a "print-out" of the amplitude distributions in those units. Thus normalized, the resulting amplitude distributions could readily be compared with published curves of various statistical processes.[1]

---

[1] For example, Nelson Wax, Editor, Selected Papers on Noise and Stochastic Processes, (New York: Dover Publications, 1954), p. 240.

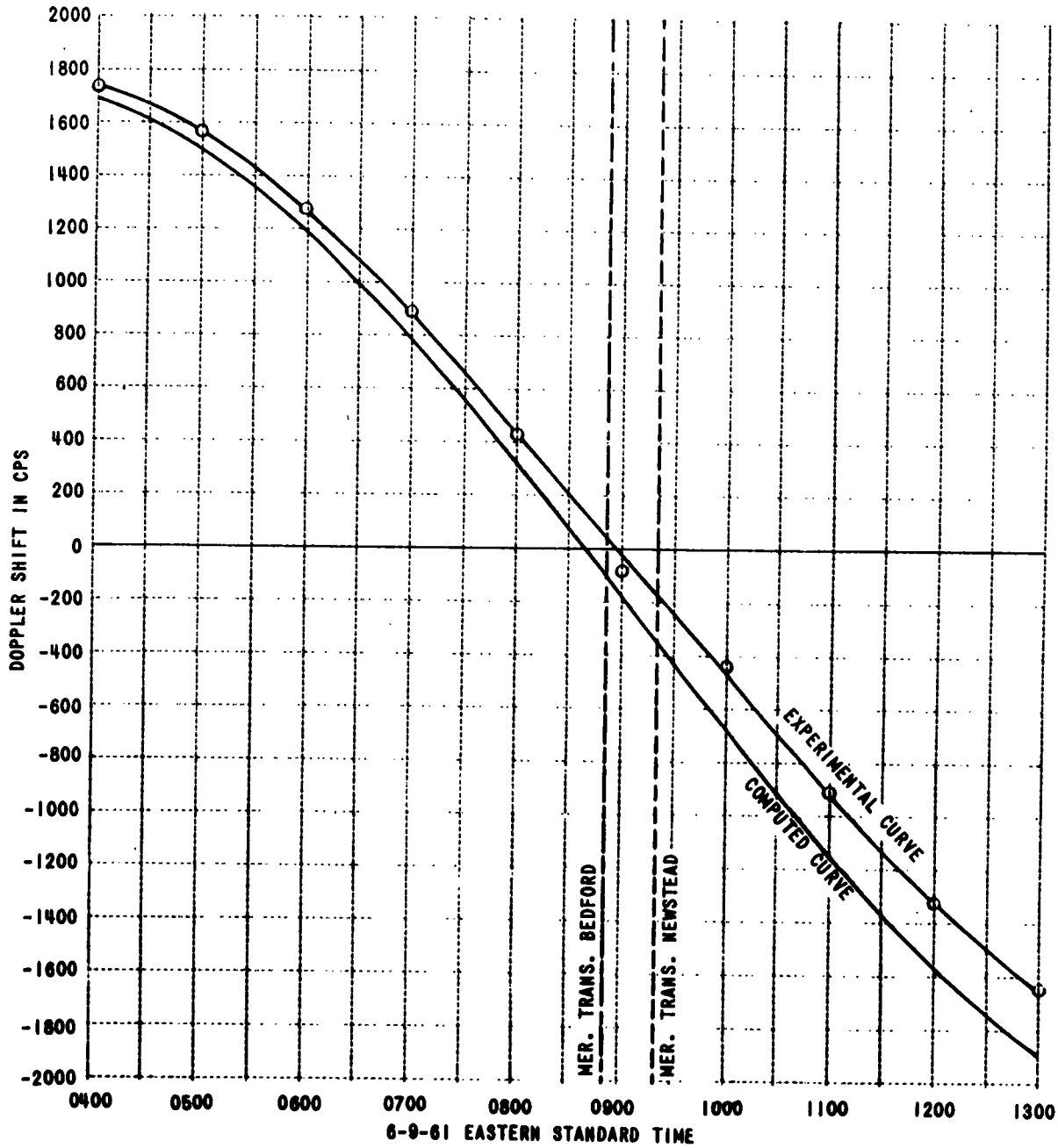

Figure 1 LUNAR DOPPLER SHIFT AT 915 Mc/S
(RECEIVER CALIBRATED AT 0145 EST)

From a total of about 100 amplitude distributions so analyzed, 85 were closely approximated by the Rice process of parameter a = 1.5 (defined in next paragraph).[1] A typical example is shown in Figures 2 and 3. One feature common to most of the histograms (a feature also shown in Figure 2) was the slow dropping-off of the amplitude distributions on the trailing edge. This feature appears frequently in statistical curves derived from propagation experiments, but no satisfactory physical explanation of the effect has been given.

The parameter a in the Rice process is by definition the ratio of sinusoidal amplitude component to the rms noise component in the composite signal. ("Noise" here refers to a random scattering process rather than thermal noise.) Consequently, when a is equal to zero, the received signal is completely random in phase and can be represented (in detected form) by the Rayleigh process. Likewise, when a approaches infinity, the received signal approaches a pure sinusoid. For a = 1.5, as observed with the moon echo, the ratio of the spectrally reflected power to the randomly scattered power in the lunar echo is equal to 1.125:1.0; the signal-to-noise ratio is 0.5 db. Another way of stating the same result is to say that, of the total power returned from the moon, 47 percent consists of randomly scattered returns, and 53 percent is a spectrally reflected signal. Thus, the rms phase error of the received signal is almost 48 degrees.

One significant feature of a lunar circuit communications link, which must be considered in the design stage, is the 10- to 90-percent fading range of the received signal. It will be noticed in Figure 3, that the theoretical fading range for the Rice (a = 1.5) process is 12.6 db. Experimentally, the "10-90" fading range was always in excess of this theoretical value and typically had a value around 14 db. This larger-than-predicted fading range may be associated with the same unknown phenomena that causes the trailing edge of the amplitude distribution histogram to decrease less rapidly than the Rice (a = 1.5) curve.

---

[1] The additional 15 samples were obviously contaminated by transmitter frequency modulation and were discarded.

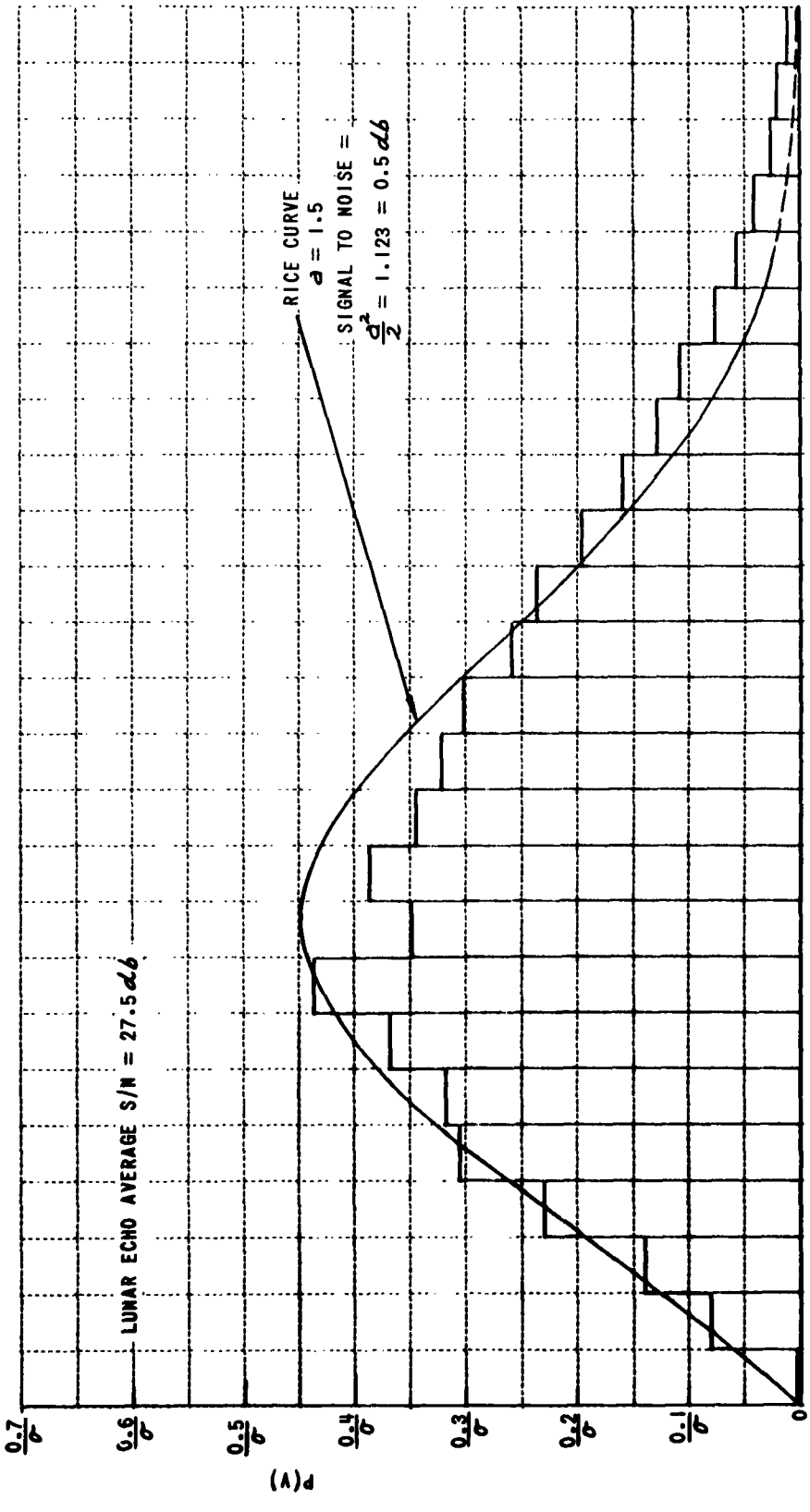

Figure 2 AVERAGE OF ELEVEN 5-MINUTE AMPLITUDE DISTRIBUTIONS
(5-10-61: 0400 TO 1500 EST)

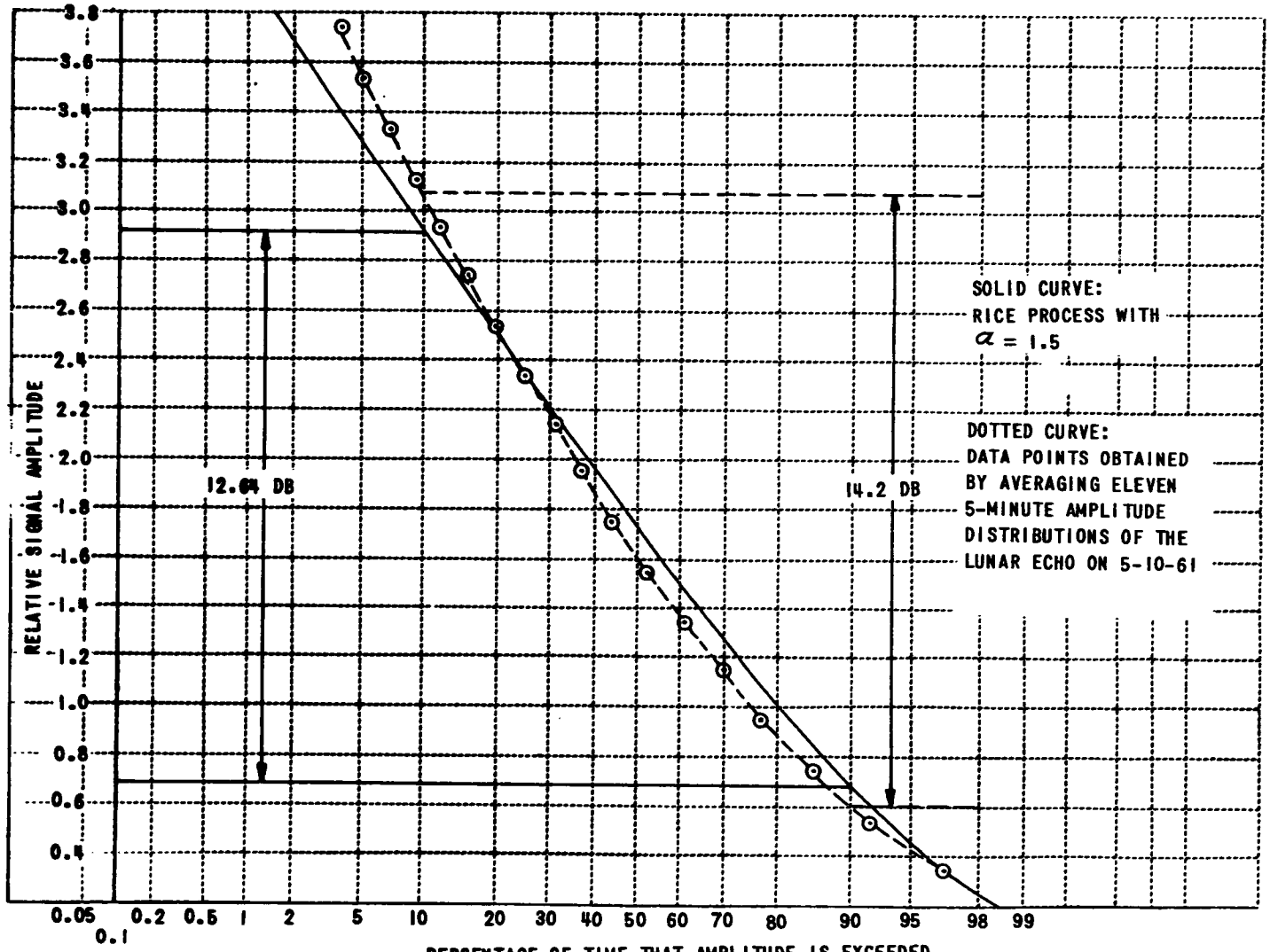

Figure 3 CUMULATIVE DISTRIBUTION OF LUNAR ECHO

It will be recalled that the mean value of detected output was obtained during the computation of lunar-echo amplitude distributions. After each 5-minute amplitude data recording, the receiving equipment was detuned, and the detected receiver noise was recorded. Thus, a mean value of the noise level was also obtained. Because equipment tests have shown a linear response of the 100-kc detector output to an input voltage at 915 mc,[1] the mean signal-to-noise ratio was computed from the mean values of detected lunar echo and receiver noise. In Appendix A, the mean value of detected noise power output from the receiving equipment is shown to be -186 dbw. It is also pointed out that periodic measurements of the noise-figure were conducted to assure that this noise level remained within ±1 db of -186 dbw. Thus, on the basis of a known noise level and the experimentally obtained signal-to-noise ratio, the transmission loss over the Bedford-Moon-Newstead path was computed.

The transmission loss between two isotropic radiators is defined as

$$TL = \frac{(4\pi)^3 r^4}{\sigma \lambda^2}$$

where σ is the radar cross section of a scattering target, λ is the free-space wavelength (equal to 0.328 m at 915 mc), and r is the distance to the scattering target. From the radar equation, it follows that

$$P_R = P_T G^2 \left(\frac{1}{TL}\right)$$

where P_R and P_T are the received power and the transmitted power respectively, and G is the antenna gain (identical receiving and transmitting antennas are assumed). If P_R/N_0 is the signal-to-noise ratio, then as long as the transmitter power remains reasonably fixed, the expression ($P_T G^2/N_0$) is a constant, amounting to 302 5 db for antenna gains[2] of 38.25 db each and a transmitted power of 10 kw. Thus, the transmission loss is the difference between

---

[1] Figure 28. Appendix A.

[2] Compared to an isotropic radiator

the signal-to-noise ratio and 302 5 db Figure 4 shows the signal-to-noise ratios obtained and the transmission losses computed during April and May 1961 The data were usually recorded every second day throughout the lunar cycle.

In Figure 5 all the signal-strength data collected during the contract performance period are plotted as a function of cumulative probability of occurrence The resulting plot is well approximated by a straight line It appears, therefore, that the experimentally obtained signal-to-noise ratios (in db) are normally distributed. From the mean value in Figure 5, the transmission loss is determined to be 279 7 db, with an rms error (one standard deviation) of 3 9 db.

Because the moon is in an elliptical orbit about the earth, it is to be expected that the transmission loss will change by about 2 5 db between the dates of lunar perigee and lunar apogee Likewise, a maximum experimental error of 4 db resulting from transmitted power uncertainty (±1 db) and receiver noise level uncertainty (±1 db) can be expected in these measurements Thus, if all these errors should add (the worst condition possible), the maximum observed variation in the signal-to-noise ratio should be no larger than 6. 5 db. The experimental data presented in Figures 4 and 5 vary by as much as 12 db. It is difficult to conceive that variations in excess of the 6. 5 db are caused by poor experimental performance alone. Consequently, the possibility exists that loss mechanisms are involved which have not been considered in this analysis.

2 Transmission Loss and Lunar Surface Scattering Properties

The second experimental task was the collection of data suitable for spectrum analysis of the lunar echo It was shown in the previous section that the statistical nature of the lunar echo does not differ much from that of band-limited noise The video spectrum of such a signal would be a convolution of the r-f spectrum[1] and would not be suitable for comparison with theoretically computed contours of constant Doppler shift on the lunar surface unless the

---

[1] Uhlenbeck, G. E. and Lawson. J. L., Threshold Signals, (New York: McGraw-Hill Book Co., Inc., 1950). Radiation Laboratory Series, Vol. 21.

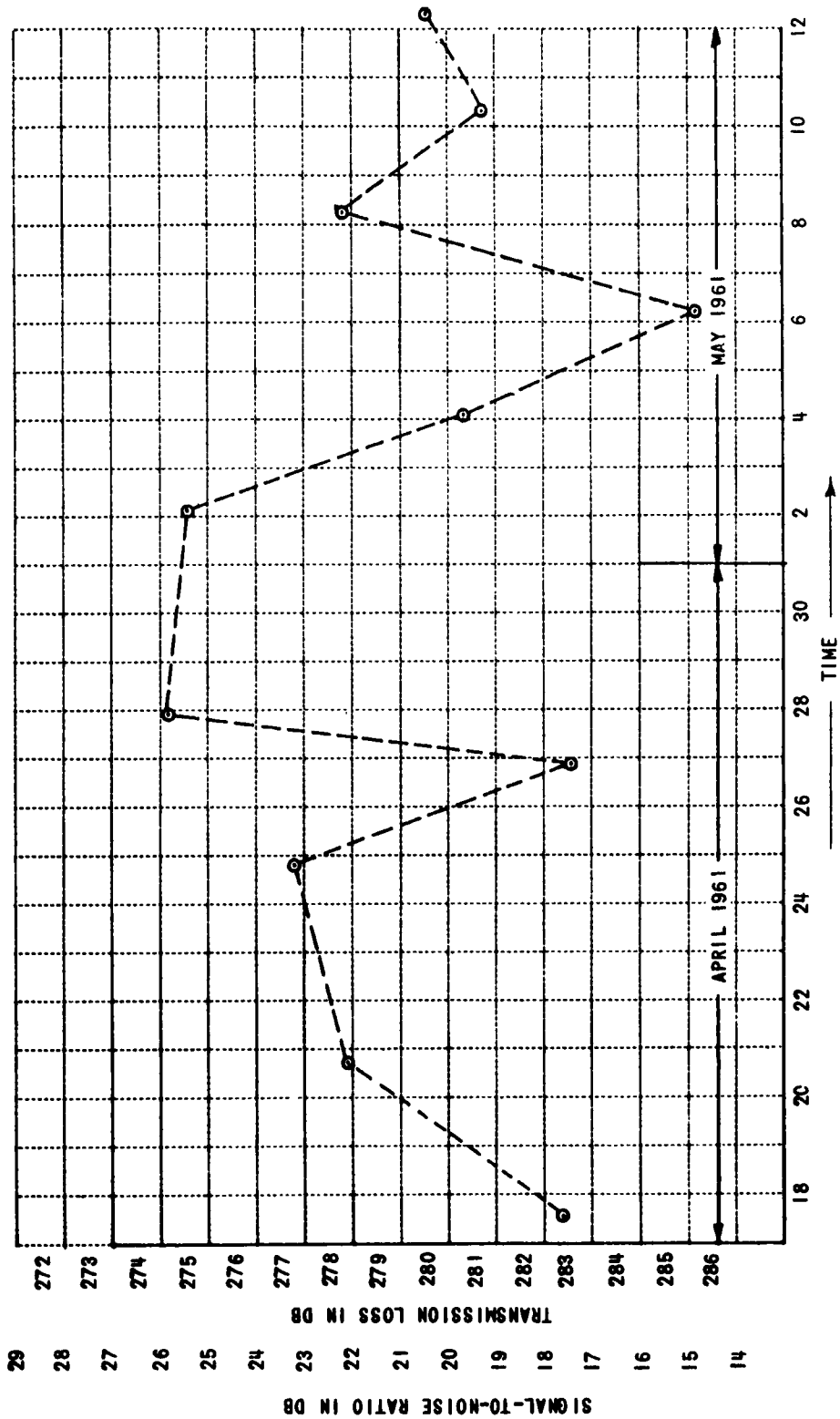

Figure 4 LUNAR ECHO - SIGNAL-TO-NOISE RATIO AND TRANSMISSION LOSS MEASURED OVER ONE LUNAR CYCLE PATH: BEDFORD-MOON-NEWSTEAD

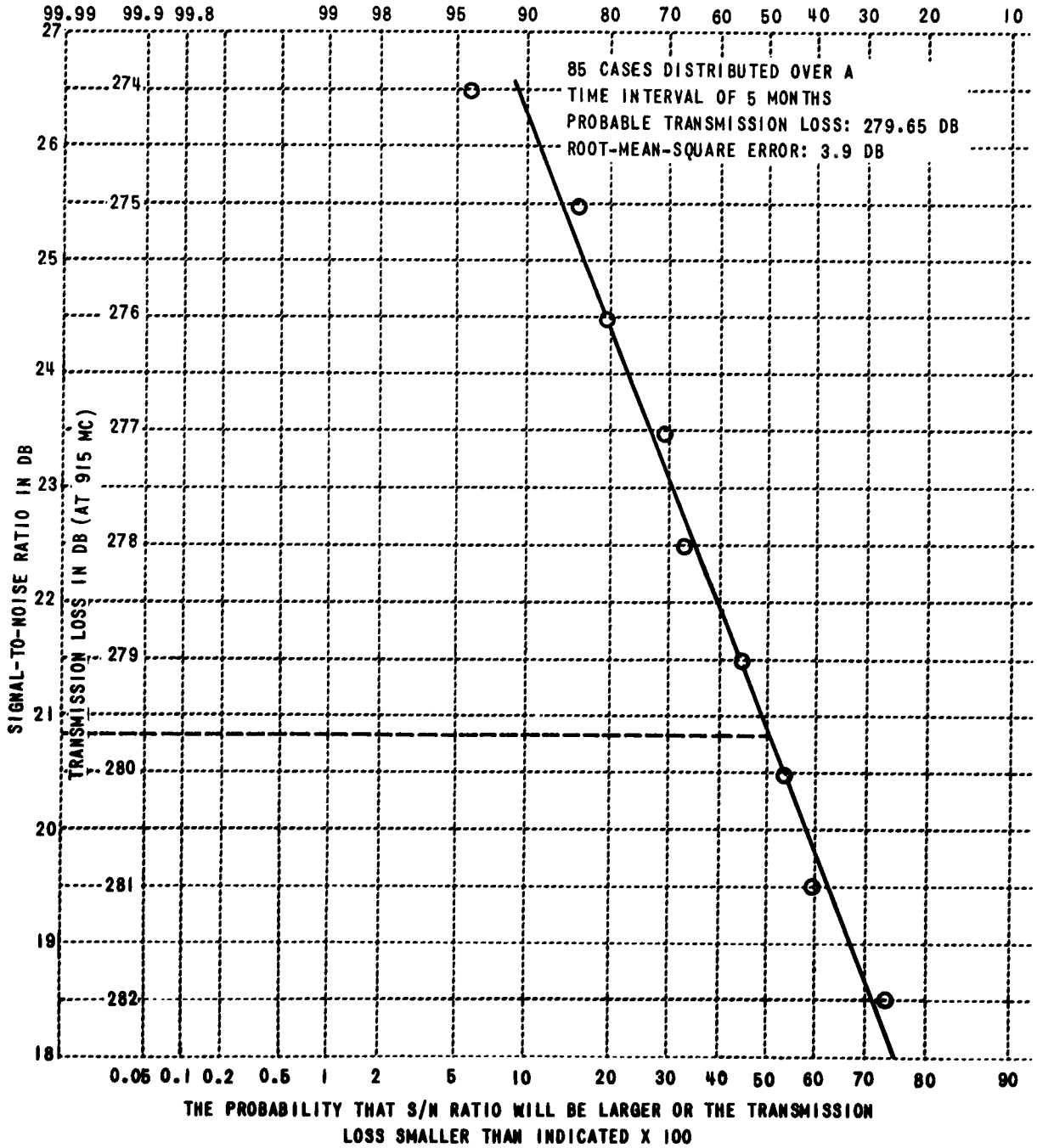

Figure 5 LUNAR ECHO SIGNAL-TO-NOISE RATIO AND TRANSMISSION LOSS PLOTTED AS A FUNCTION OF PROBABILITY OF OCCURRENCE

lunar echo spectrum were symmetrical about the carrier frequency. The consequences of the detection process had to be eliminated from the experimental data collected. The technique used to obtain the lunar echo spectrum is illustrated in Figure 22 (Appendix A). Typical lunar echo spectra thus derived are illustrated in Figure 6.

The data used to obtain these spectra were recorded at 1-7/8 inches per second on magnetic tape, and each spectrum consisted of a 30-second sample of the lunar echo. Sample times in excess of 30 seconds were found impractical because the mean Doppler frequency changes at a rate of approximately 1.6 cps per minute; therefore, the spectrum broadening during a 30-second interval is 0.8 cps, a value comparable to the frequency resolution of this data reduction technique. The recorded data were continuously played back at 60 inches per second into a spectrum analyzer, and the resulting display on the cathode-ray oscillograph was photographed for 10 minutes. Frequency calibration of the spectrum analyzer was accomplished by the use of a control signal channel on the magnetic tape. Recorded on this control channel (at 1-7/8 in./sec) were three accurately known sine-wave voltages at 190 cps, 200 cps, and 210 cps. Before reduction of the lunar echo data, the control signals were played back at 60 inches per second, and the frequency deviation of the spectrum analyzer was adjusted so that the 190-cps and 210-cps signals coincided with the horizontal extremes of the calibration grid.

For each lunar echo spectrum obtained, a lunar surface map which contained contours of constant Doppler shift was computed. The details of this computation are set forth in Appendix D, and an example of such a map is shown in Figure 7. It will be observed in Figure 7 that the contours of constant Doppler shift appear as straight lines. In reality, the lines are hyperbolae, which, over the small central area on the moon, are adequately approximated by straight lines. It will, furthermore, be noticed that the contours of constant Doppler shift are inclined to the lunar equator. The angle of contour inclination, as well as the amount of contour separation (in cps per degree of lunar latitude), changes from day to day and completes a cycle roughly every 28 days. The change of the contour separations as a function of time is illustrated in Figure 8.

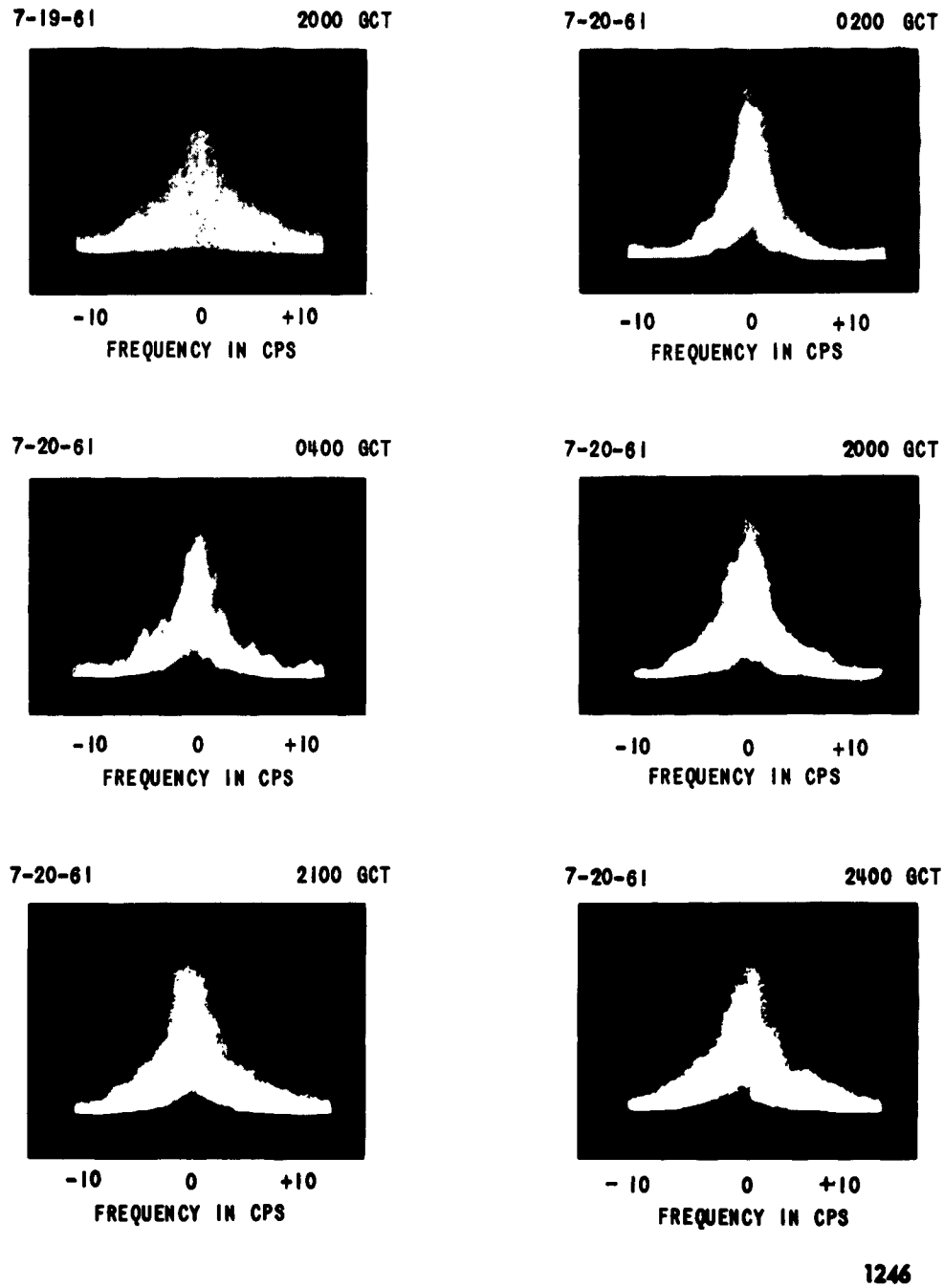

Figure 6 TYPICAL LUNAR ECHO SPECTRA

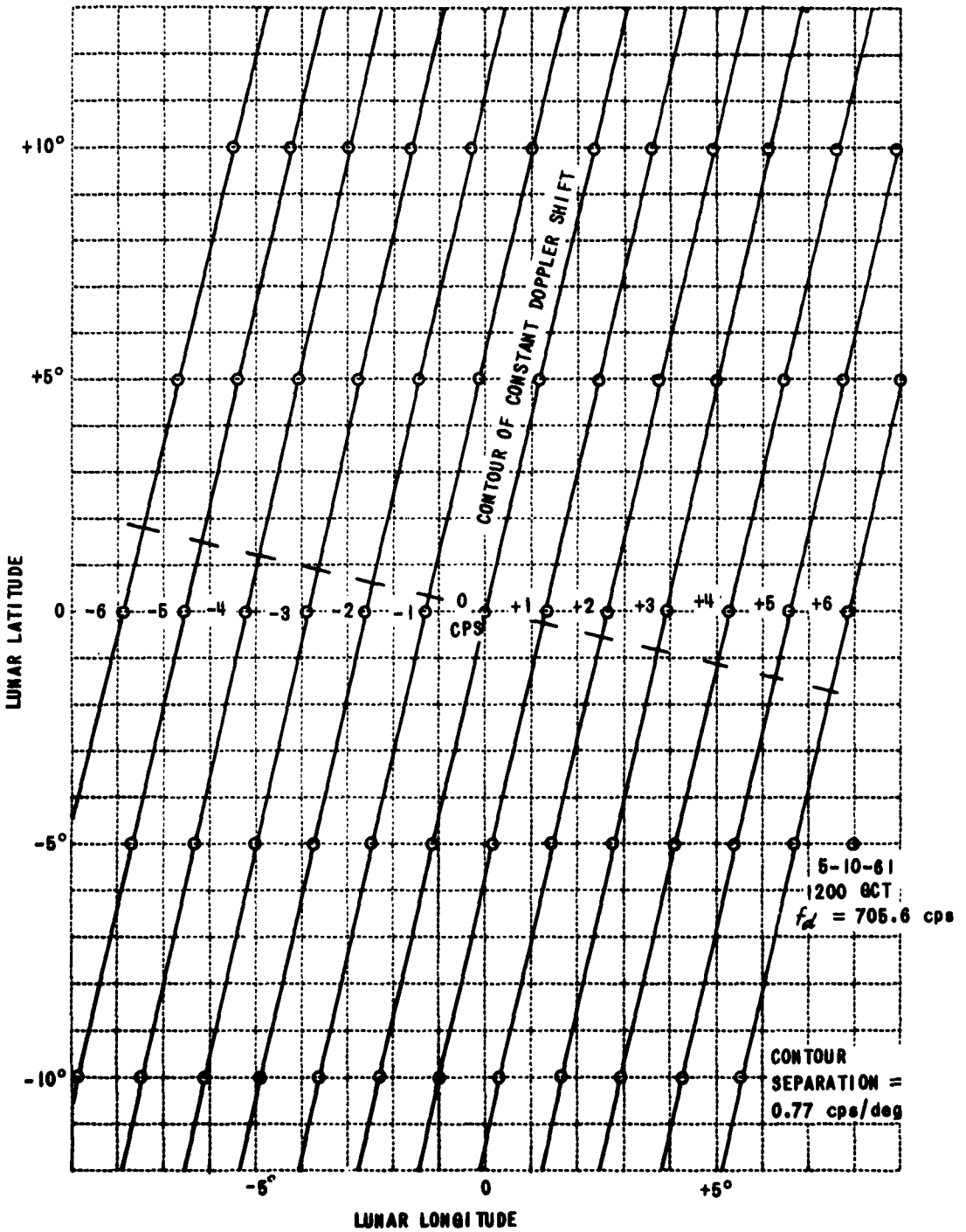

Figure 7 EXAMPLE OF COMPUTED CONTOURS OF CONSTANT DOPPLER SHIFT PLOTTED IN LUNAR COORDINATES

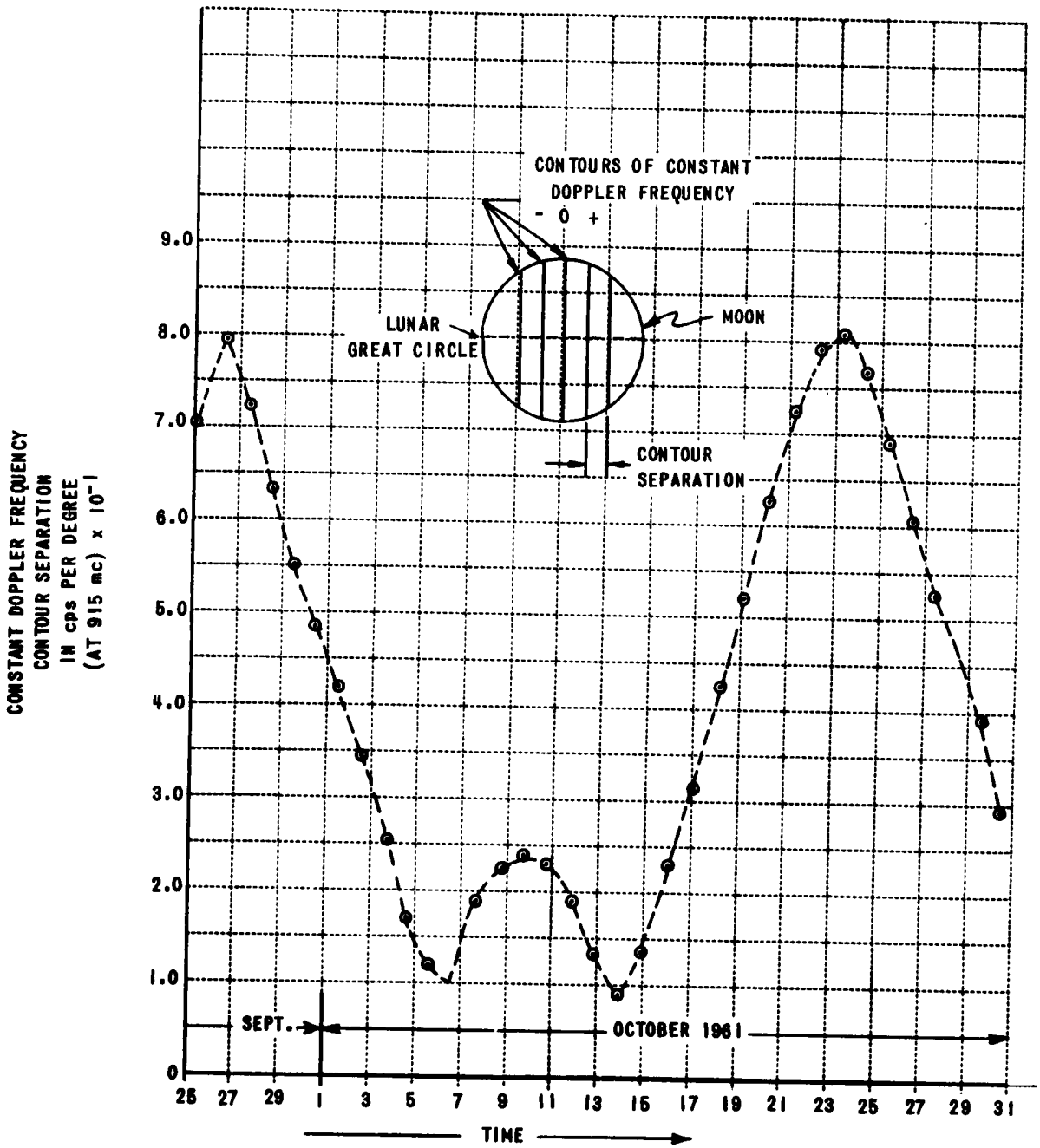

Figure 8 CONSTANT DOPPLER FREQUENCY CONTOUR SEPARATION AS A FUNCTION OF TIME

The experimentally determined spectra are plots of lunar echo amplitude as a function of frequency. This information by itself cannot be used to determine the scattering properties of the moon. However, in conjunction with the knowledge of where contours of constant Doppler shift are located on the lunar surface, it is possible to convert the basic data from amplitude-versus-frequency to amplitude-versus-reflection angle (i.e. the angle between the reflected ray and the lunar radius vector at the scattering point). In addition to carrying out this conversion, the areas under the lunar echo spectra were normalized to agree with the average power recorded for transmission loss data (Section 1), thus providing a basis of comparison for all the lunar echo spectra obtained from the experiment. Figure 9 is a plot of the average angular spectrum of the lunar echo. Plots of lunar range depth and time delay, integrated lunar surface area, and percentage energy returned per integrated area are presented in Figures 10, 11, 12 and 13, respectively. Each of these curves, with the exception of the one shown in Figure 13, is accompanied by a sketch that illustrates the geometry involved and the appropriate equations used. Figure 13 was constructed by plotting against lunar surface area the integrated area (normalized to 1.0) under the relative power vs. time-delay curve of Figure 10. Note that 90 percent of the total energy returned from the moon comes from an area of about 13×10^{10} square meters, corresponding to a range depth (see Figure 10) of about 80 microseconds, or 12 kilometers. Of particular interest in Figure 13 is the dotted rectangle, the area of which is equal to the hatched area over the percent-total-energy curve. The dotted rectangle intersects the x-axis at a value of lunar surface area, which, if all the energy incident upon it were reflected, would lead to the same transmission loss over the earth-moon-earth circuit as is actually observed. This value is 4.2×10^{10} square meters.

Again, assume that the transmission loss is given by

$$TL = \frac{(4\pi)^3 r^4}{\sigma \lambda^2}$$

where $\lambda = 0.328$ meters, and the earth to moon distance $r = 3.84 \times 10^8$ meters. Substitution of 4.2×10^{10} square meters for σ results in a transmission loss of 280.2 db. It will be recalled that the transmission loss determined

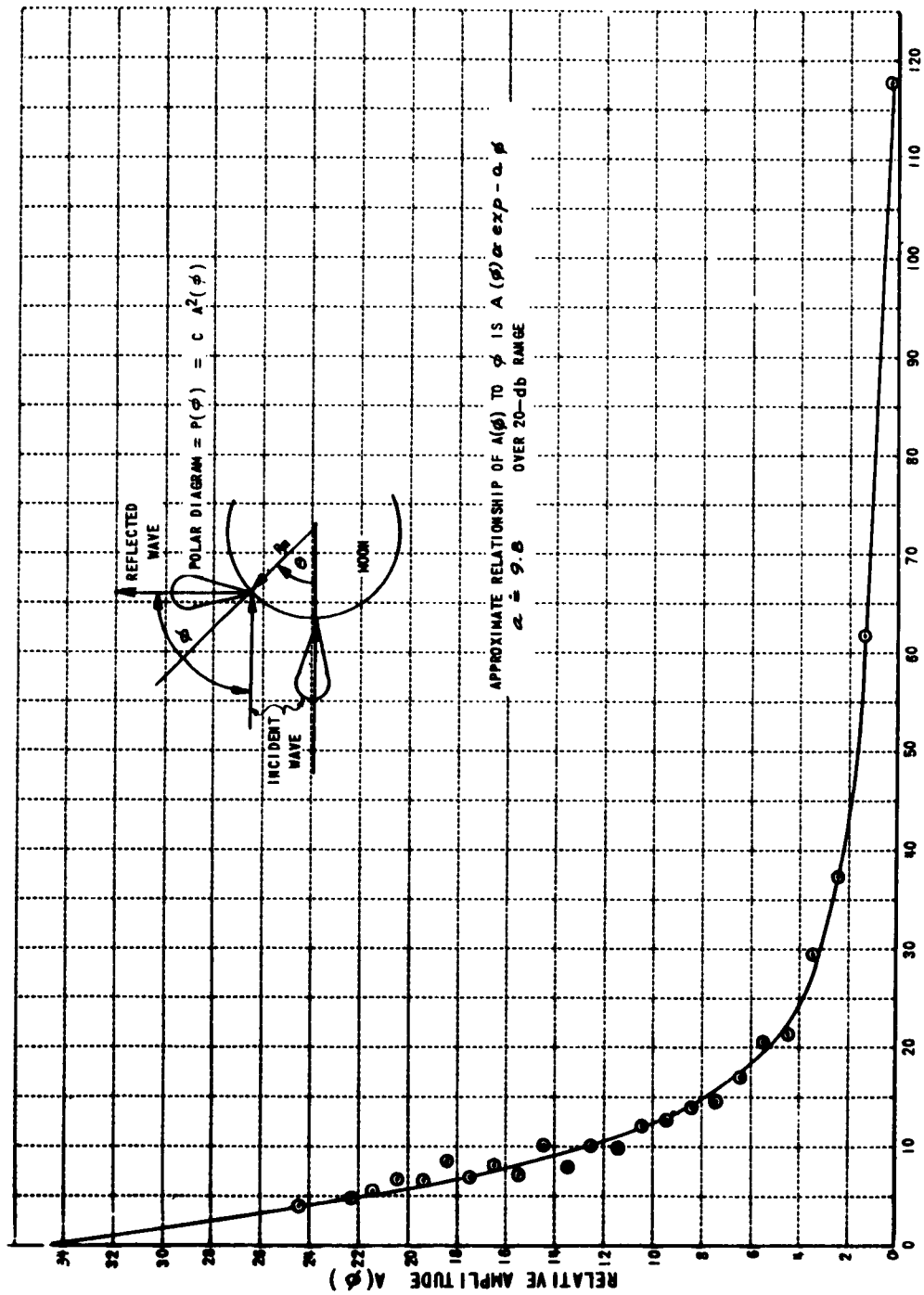

Figure 9 ANGULAR SPECTRUM OF LUNAR ECHO

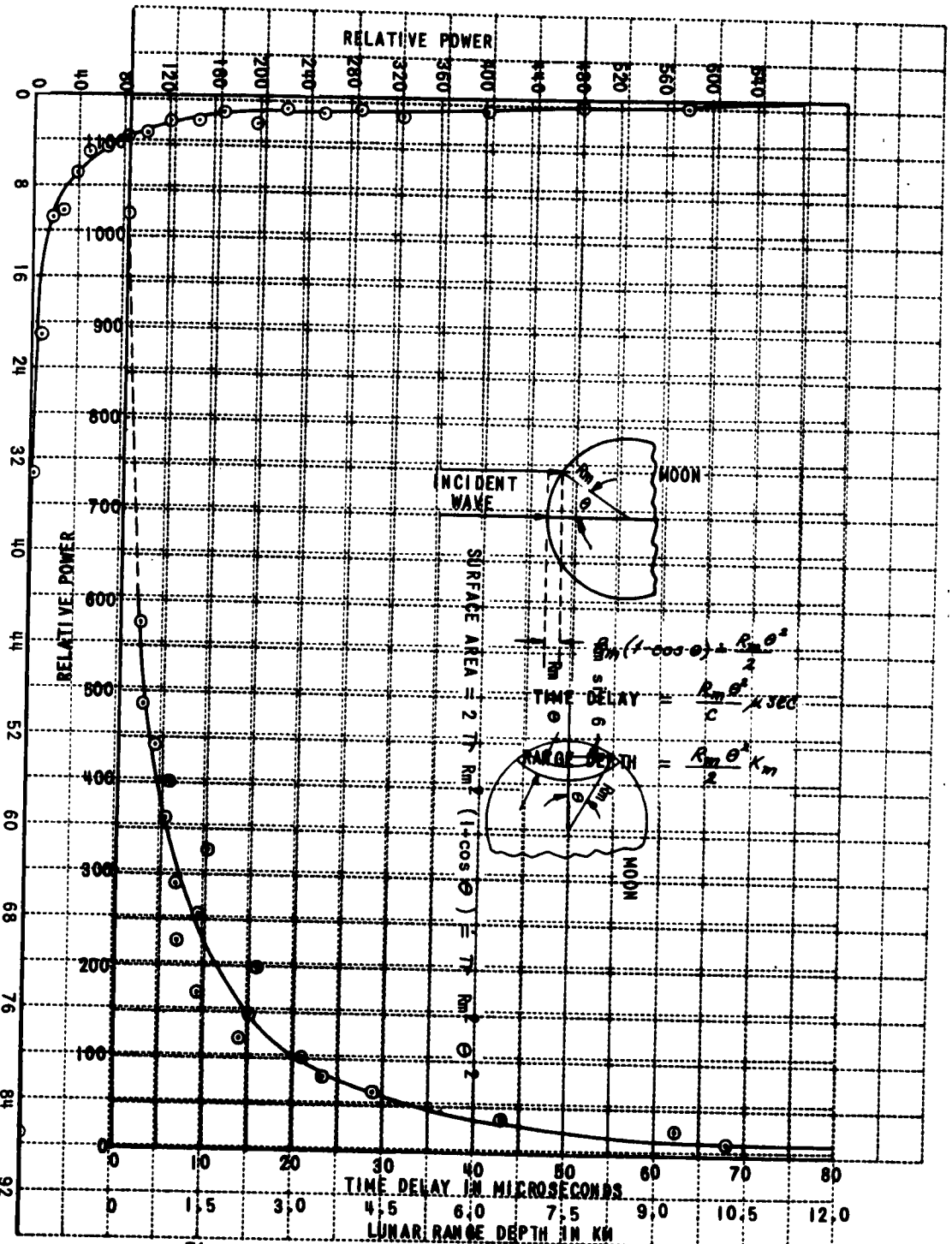

Figure 11 RELATIVE POWER AS A FUNCTION OF LUNAR SURFACE AREA

Figure 10 RELATIVE POWER AS A FUNCTION OF TIME DELAY AND LUNAR RANGE DEPTH

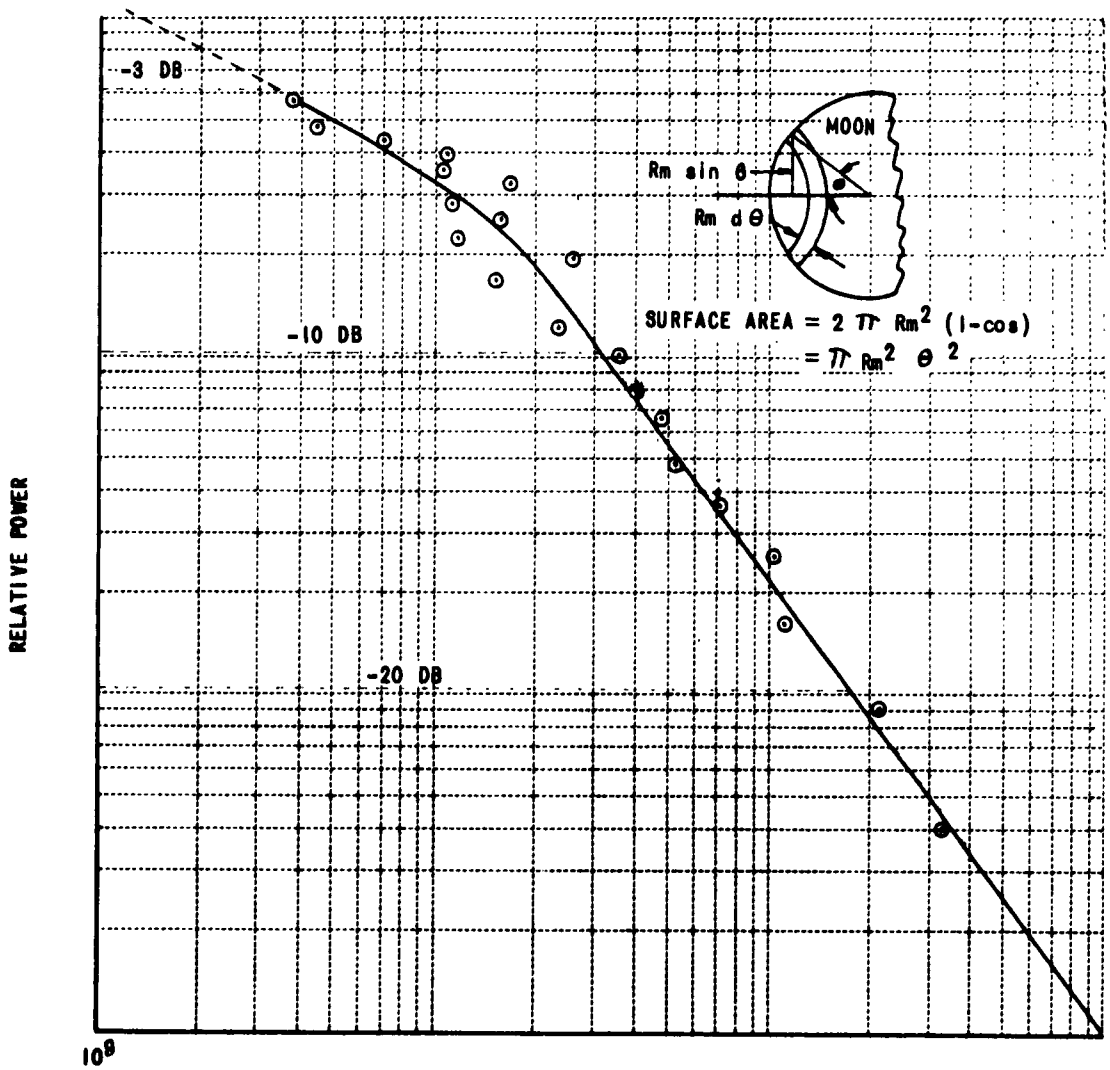

Figure 12 RELATIVE POWER AS A FUNCTION OF LUNAR SURFACE AREA (LOGARITHMIC PLOT)

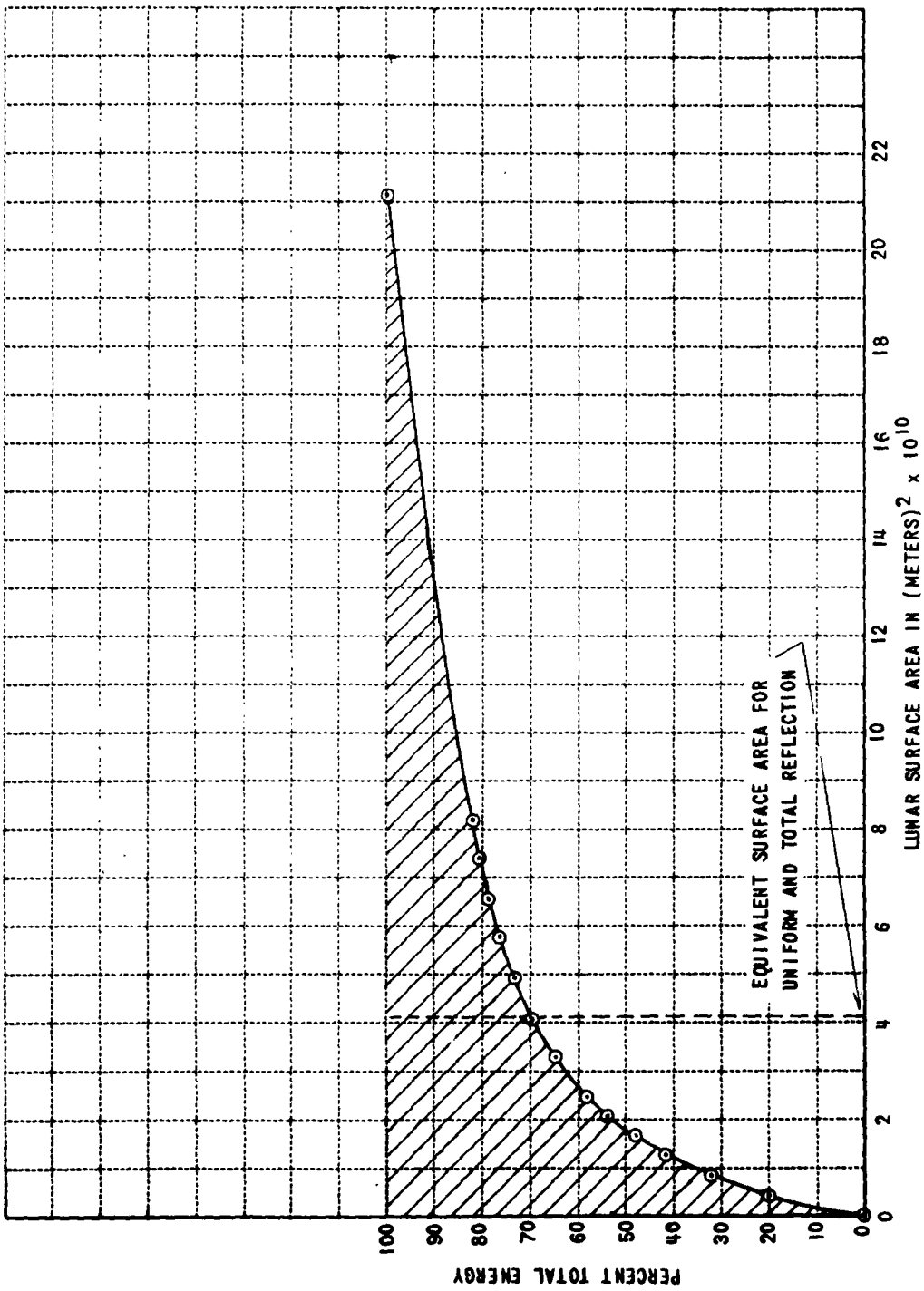

Figure 13 PERCENT TOTAL ENERGY AS A FUNCTION OF LUNAR SURFACE AREA

in Figure 5 was 279.7 db. These two values differ by only 0.5 db and thus substantiate the two independent methods used to arrive at the resulting transmission loss. Further substantiation of the transmission loss at 915 mc is given in Figure 14, where transmission loss data over the earth-moon-earth link obtained at other frequencies by various investigators[1, 2, 3, 4] are plotted. Even though accuracies of no better than 4 db are claimed for any of these points, it is interesting to note that the transmission loss appears to increase at a constant rate of 12.8 db per octave in the frequency interval of 200 mc to 3000 mc. From the data presented here, there seems to be no substantiation of Trexler's[1] assumption that the transmission loss between 20 mc and 3000 mc increases at a rate of 6 db per octave, an assumption implying that the moon's radar cross section does not change with frequency. In fact, the data shown in Figure 14 indicate that the reflection characteristic of the moon is frequency dependent because the transmission loss increases by 12.8 db instead of 6 db per octave. Therefore, by virtue of the additional transmission loss of 6.8 db per octave, it must be concluded that the radar cross section (between 200 mc and 3000 mc) of the moon is roughly proportional to the square of the wavelength.

It is tempting to speculate regarding the mechanism that could give rise to that observation. Even though the data presented in Figure 14 are well approximated by a straight line, it would seem reasonable that at lower frequencies than those indicated, the slope will change. This break point in the curve will correspond to a "corner frequency" f_o, an analogy for which would be the 3-db point in the response of a low-pass R-C filter. If it is further assumed that the

---

[1] Trexler, J. H., "Lunar Radio Echoes," Proc. IRE, 46, 286-292 (1958).

[2] Yaplee, B. S., et al., "Radar Echoes from the Moon at a Wavelength of 10 Cm," Proc. IRE, 46, 293-297 (1958).

[3] Ingalls, R. P., et al., Bandpass Measurements of a Lunar Reflection Circuit, Lincoln Laboratories Report 33G-0011, January 26, 1961.

[4] Ingals, R. P., et al., A Study of Space Communications through an Aurora Using the Moon as a Reflector, Lincoln Laboratories Report JA-1350, February 25, 1960.

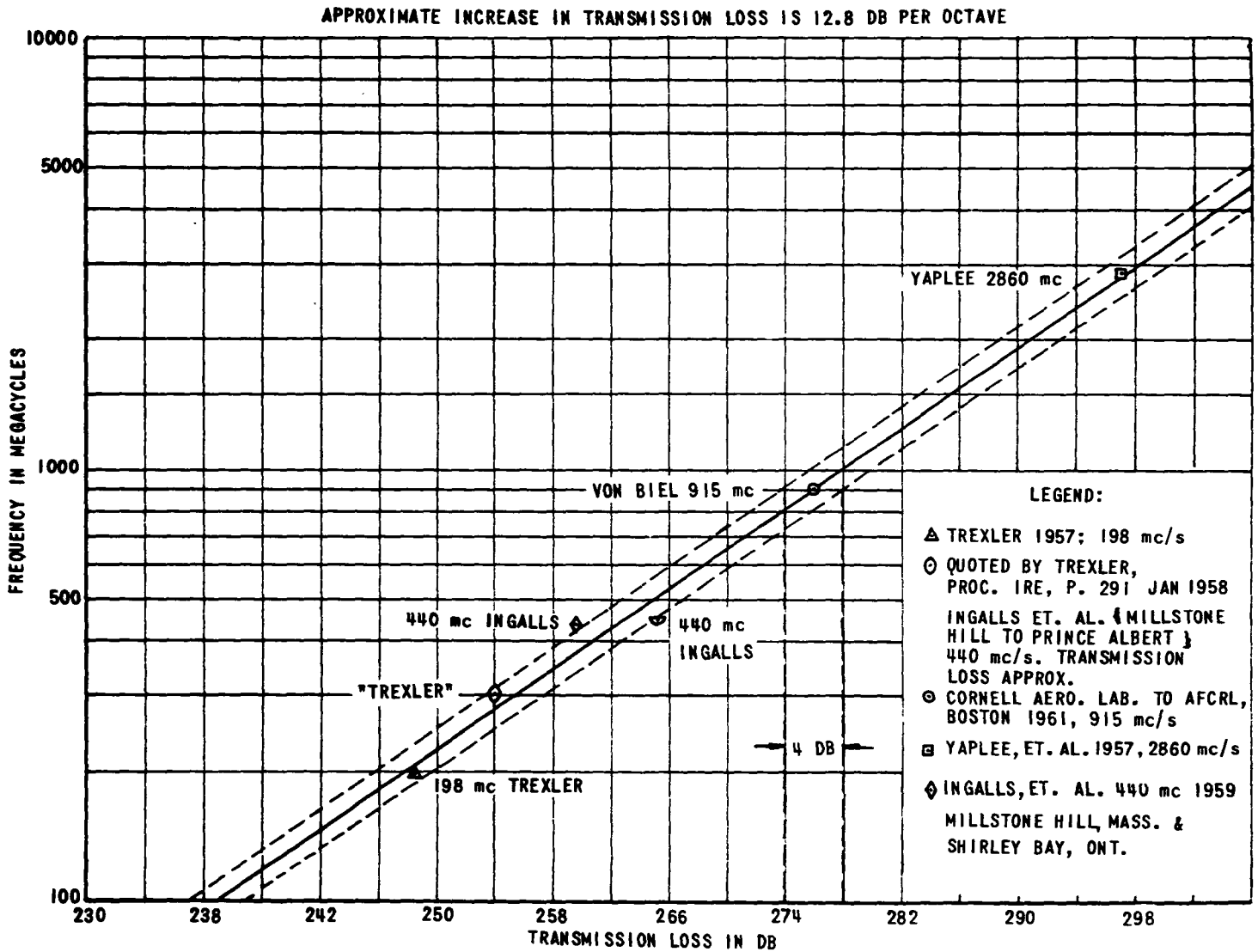

Figure 14 LUNAR CIRCUIT TRANSMISSION LOSS BETWEEN ISOTROPIC RADIATOR AND COLLECTOR AS A FUNCTION OF FREQUENCY

moon's radar cross section can be described by

$$\sigma(k) = C\left[\frac{1}{1+(k/k_0)^2}\right]$$

where $k = \frac{4\pi}{\lambda}$ (for the backscatter case)
and $C = 9.5 \times 10^{12}$ meters^2 (the geometrical cross sectional area of the moon), then, with the aid of the radar cross section determined experimentally at 915 mc, λ_o is found equal to about 5 meters, and the correlation distance on the moon (equal to $\frac{\lambda_o}{2}$) is about 2.5 m. This result, though based purely on speculation, should bear some relationship to the angular spectrum observed experimentally. On the assumption that the correlation distance on the moon is 2.5 m, the amplitude of the returned echo at 915 mc (Figure 9) should have decreased to $\frac{\sqrt{2}}{2}$ of its maximum value when the angle ϕ is about 3.3×10^{-2} radians. In reality, the amplitude of the echo is down to $\frac{\sqrt{2}}{2}$ of the maximum value when ϕ is 4.0×10^{-2} radians. This value of ϕ results in a correlation distance of approximately 2.0 meters.

Because the assumptions made in the derivation of these values for the correlation distance on the moon do not permit accuracies greater than one order of magnitude, it may be concluded only that the scale size of the scattering irregularities on the lunar surface is on the order of 1 meter.

3. Faraday Rotation

The technique used to record polarization data is outlined in Appendix A and is illustrated in Figures 25 and 26. During polarization measurements, the feed horn was continuously rotated. Thus, cross polarization of the receiving antenna with the incoming signal occurred twice for every revolution of the feed horn. The average of twenty cross-polarization points was used to determine each experimental value of the lunar echo polarizations. For Figures 15, 16 and 17, polarization data points were obtained every half hour from moonrise to moonset. All three figures exhibit the same general shape, the major difference being that the maximum value of the polarization in Figure 16 is only about one-half that in Figures 15 and 17. Assuming that the polarization changes observed are caused by Faraday rotation, the polarization angle ρ can be represented approximately by

$$\rho = k \sec \theta \int_0^h N(z) B_L(z)\, dz$$

where k is a proportionality constant, θ is the zenith angle of the propagation vector, $N(z)$ is the electron density, and $B_L(z)$ is the component of the earth's magnetic field parallel to the direction of propagation. Since the three curves present data collected on three successive days, the moon's declination did not change sufficiently to account for a change of a factor of two in either $\sec \theta$ or $B_L(z)$ or the product of the two. It must be concluded that the integrated electron density $\int^h N(z)\, dz$ was responsible for this change. Polarization observations were also made at lunar meridian transit every second day over an interval of one lunar cycle. The results plotted in Figure 18 indicate that the integrated electron concentration over the entire transmission path did not vary by more than about 40 percent. From these results it must be concluded that at 915 mc, polarization changes of about 50 degrees frequently occur over the lunar transmission path. This amount of polarization rotation will cause a signal strength deterioration in excess of 3 db if left uncompensated.

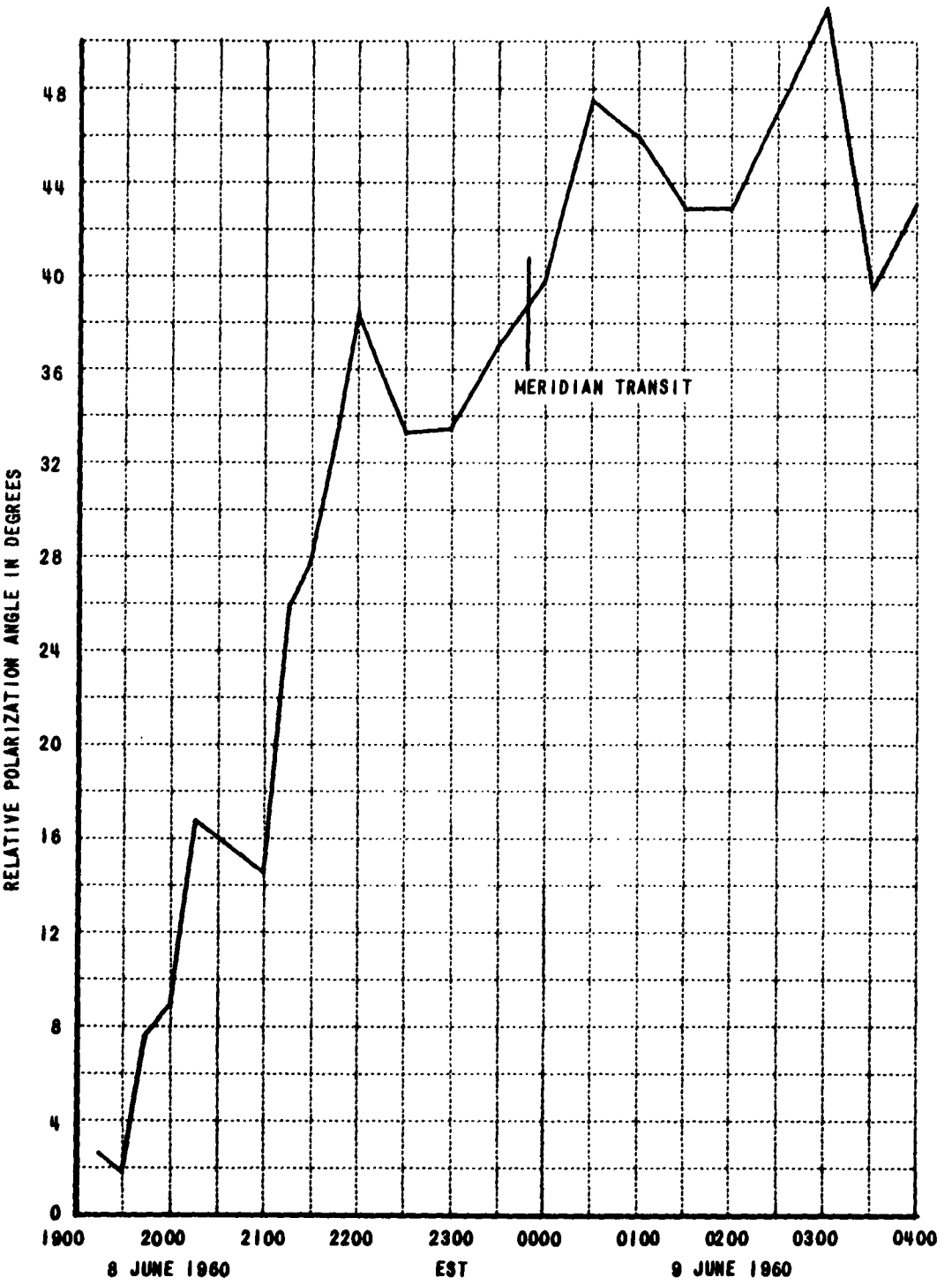

IP479-10

Figure 15 DIURNAL VARIATION OF THE LUNAR ECHO POLARIZATION
8 - 9 JUNE 1960

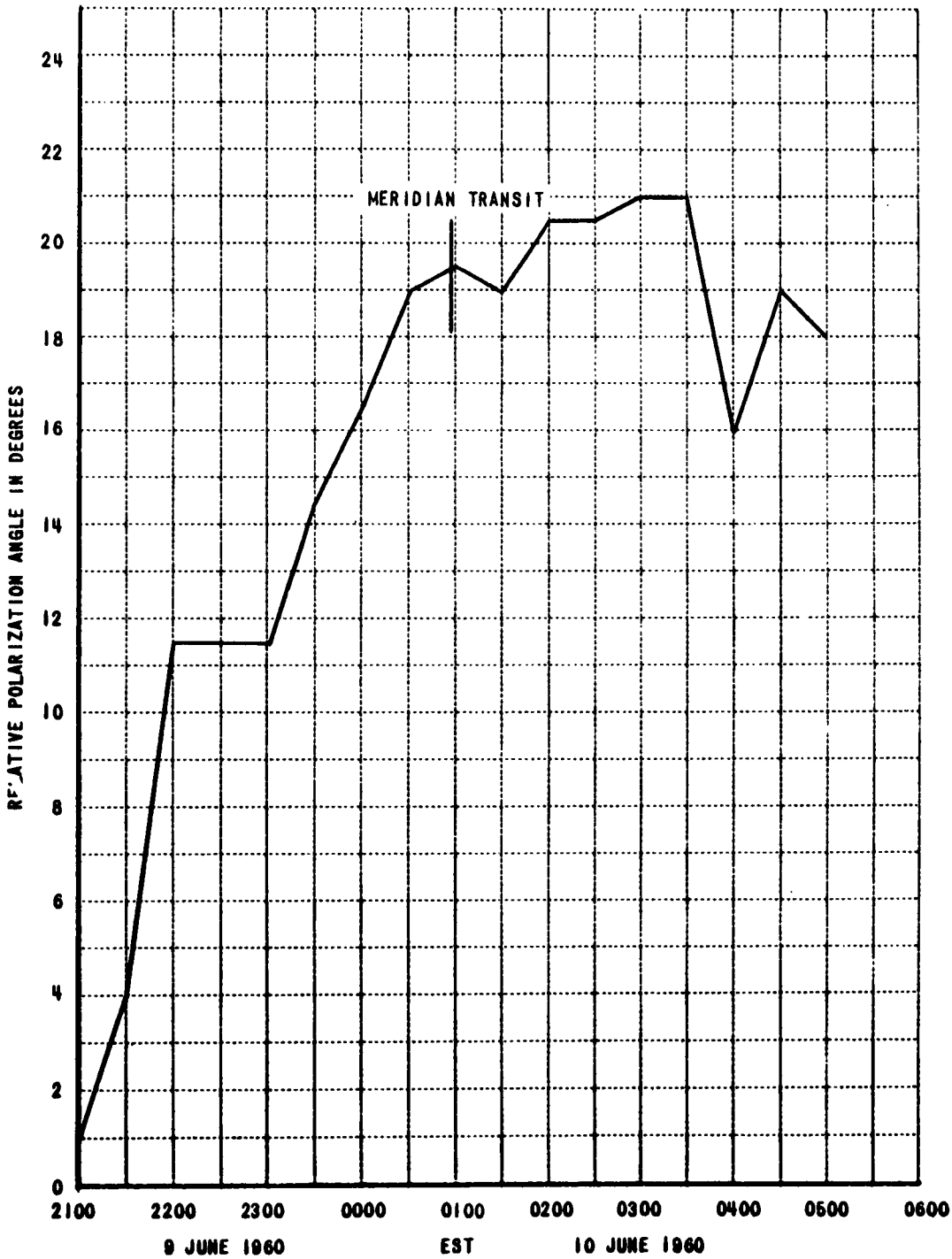

Figure 16 DIURNAL VARIATION OF THE LUNAR POLARIZATION
9 - 10 JUNE 1960

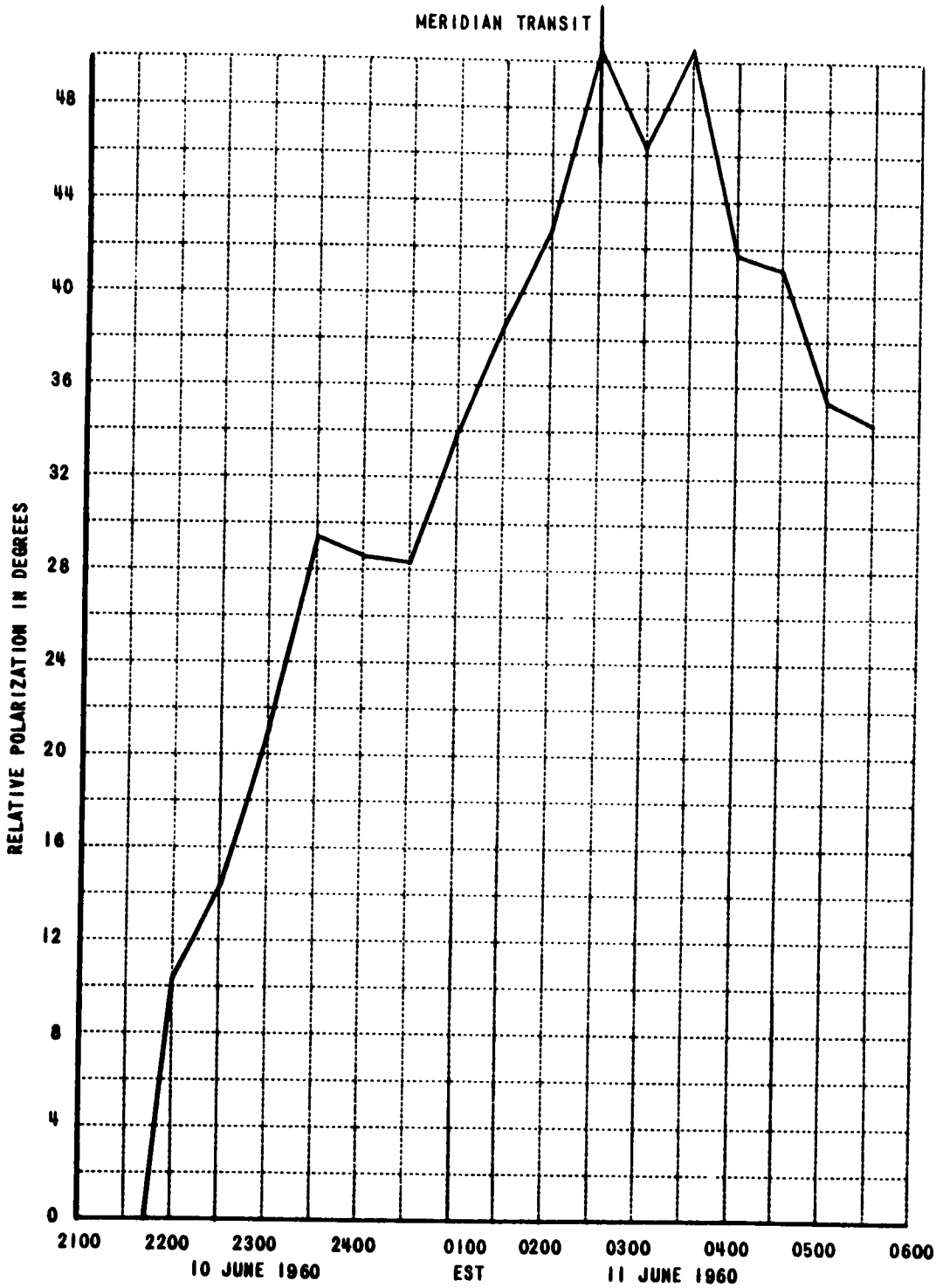

Figure 17 DIURNAL VARIATION OF THE LUNAR ECHO POLARIZATION
10 - 11 JUNE 1960

IPA79-12

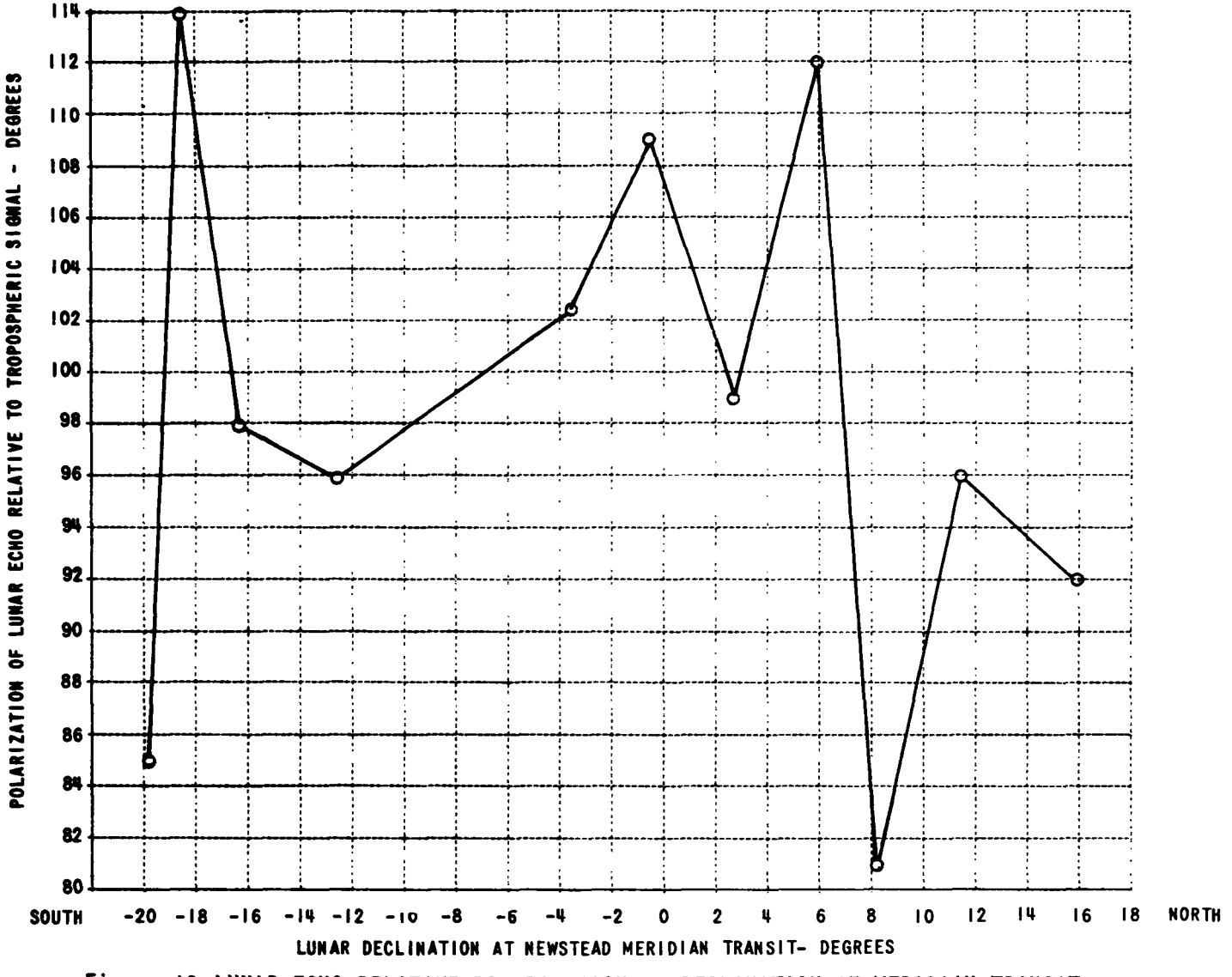

Figure 18 LUNAR ECHO RELATIVE POLARIZATION VS DECLINATION AT MERIDIAN TRANSIT
(NEWSTEAD)

IV. SUMMARY

The lunar echo experiment was designed to provide basic data for a possible earth-moon-earth communication circuit at 915 mc. Specific questions to be answered concerned the transmission loss to be expected over the circuit, the statistical nature of the lunar echo, the scattering properties of the lunar surface, and the effect of the earth's ionosphere on signal polarization.

The transmission loss and the statistical nature of the lunar echo were determined from amplitude distribution data. The results obtained indicated a transmission loss of 280 db and a near-random statistical process that can be adequately approximated by the Rice process for which a = 1.5.

The scattering properties of the lunar surface were obtained by a less direct method than any of the previous experimental investigations. To accomplish this last experiment, the frequency spectrum of the lunar echo was determined experimentally. Subsequently, the Laboratory-owned IBM 704 computer was used to relate the experimentally obtained frequencies to contours of constant doppler shift on the lunar surface. The results from this computation, in conjunction with the lunar echo spectra, were used to determine the angular spectrum of the scattering areas on the moon. Further use was made of the same data to compute the moon's radar cross section and transmission loss at 915 mc. Again, a transmission loss of 280 db was obtained.

The transmission loss determined at 915 mc was compared with values of transmission loss obtained by other investigators at frequencies between 200 mc and 3000 mc. All the data thus compared indicate that the transmission loss increases with frequency at a rate of about 12 db per octave. Because the transmission loss between any two points is inversely proportional to λ^2 and thus increases at a rate of 6 db per octave, it was concluded that the moon's radar cross section is proportional to λ^2 and must decrease with increasing frequency at a rate of 6 db per octave to be in accord with the experimental results.

Polarization measurements were conducted by recording the polarization of the receiving antenna feed at cross polarization. These measurements indicated polarization changes as large as 50 degrees over a ten-hour time interval with random day-to-day variations in the signal polarization (at local meridian transit) in excess of 30 degrees. Because no observable correlation was found between the polarization data and the magnetic field component along the direction of propagation or the secant of the zenith angle, it must be concluded that the observed polarization changes (approximately 40 percent) were caused by changes in the integrated electron density between the moon and the earth.

The results obtained from this lunar echo experiment at 915 mc are generally in agreement with results published by other investigators. It should be pointed out, however, that our data, in conjunction with data derived from experiments between 200 mc and 3000 mc, do not substantiate Trexler's conclusion that the lunar circuit transmission loss increases at a rate of 6 db per octave.

Finally, on the basis of our experimental results, an attempt was made to establish a measure of the moon's roughness to radio waves. Our deduction that the scale size of irregularities is on the order of one meter appears to agree with all the available published results from lunar echo experiments.

APPENDIX A

EQUIPMENT

The receiving equipment used for the lunar echo experiment is located at Newstead, New York,[1] and is separated from the transmitter site in Bedford, Massachusetts,[2] by a great-circle distance of 600 km or 372 statute miles. The transmitting and receiving antennas are identically constructed 28-foot parabolic reflectors steerable in equatorial coordinates. At the operating frequency of 915 mc, the nominal beamwidth of the antennas is 2.55 degrees; their forward gain is approximately 38.5 db greater than that of an isotropic radiator.

At the transmitter site in Bedford, Massachusetts, a single modulated-anode klystron is used to deliver 10 kilowatts of c-w power to the antenna. The final output frequency of 915,001,344 cps is harmonically generated from the basic crystal frequency of 99,284 cps. This frequency is derived from a frequency standard,[3] capable of a long-term stability of one part in 10^8. Even though only c-w transmissions were required for this particular lunar experiment, the transmitter included provision for both amplitude and frequency modulation.[4]

Because the receiver located at Newstead, New York, was used for radio astronomy and auroral echo detection[5] as well as for the lunar echo experiment, special design emphasis was placed on maximum flexibility of operation. The entire receiving system is shown in the block diagram (Figure 19). Details of the physical installations are shown in Figures 20 and 21.

---

[1] Geographic position of Newstead antenna: Lat = 42° 59.4' N Long = 78° 33.8' N.

[2] Geographic position of Bedford antenna: Lat = 42° 27.8' N Long = 71° 17.5' W.

[3] Manufactured by General Radio Company, West Concord, Massachusetts.

[4] Double-sideband, suppressed-carrier amplitude modulation was used for a lunar experiment conducted by the General Electric Company under Contract AF 19 (604)-6634.

[5] The auroral echo program is described in Part II of this report.

IPA79-13

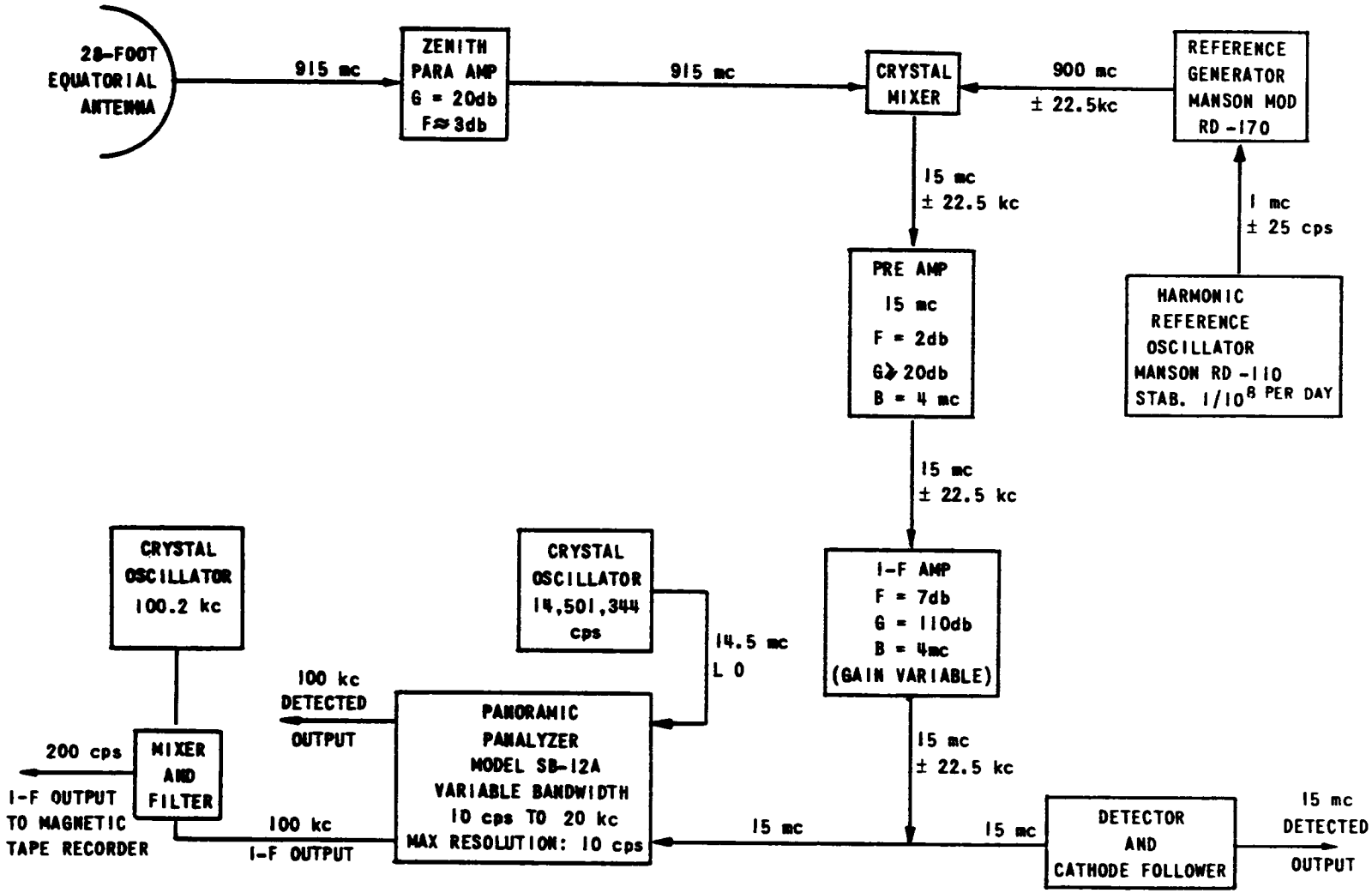

Figure 19 LUNAR AND AURORAL ECHO RECEIVER, BLOCK DIAGRAM

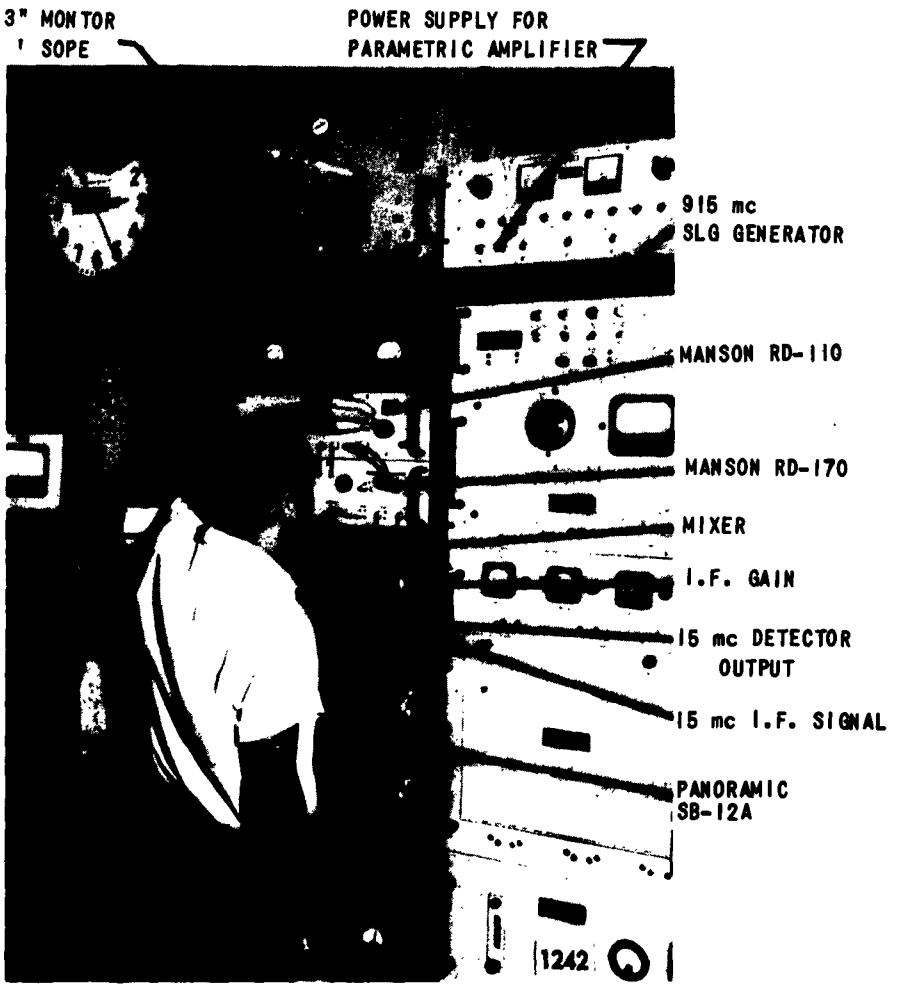

Figure 20 RECEIVER CONSOLE

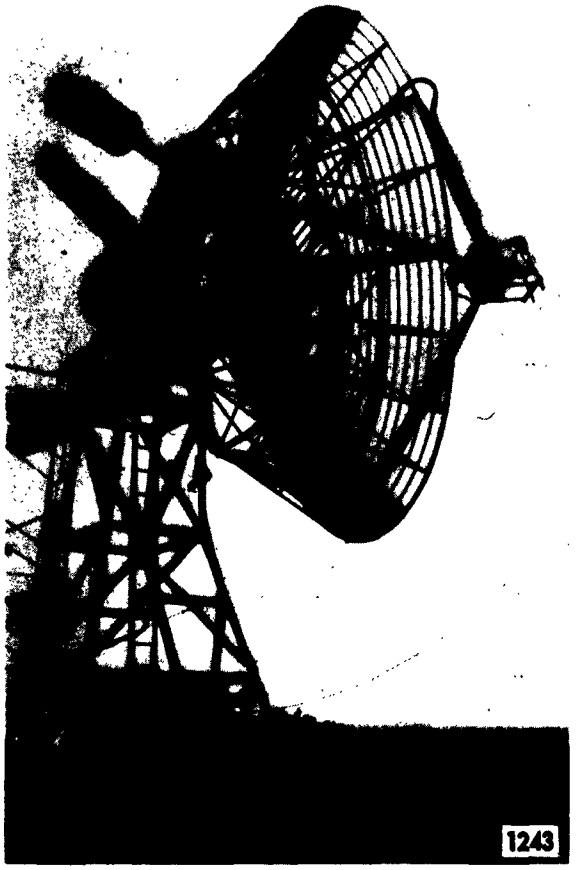

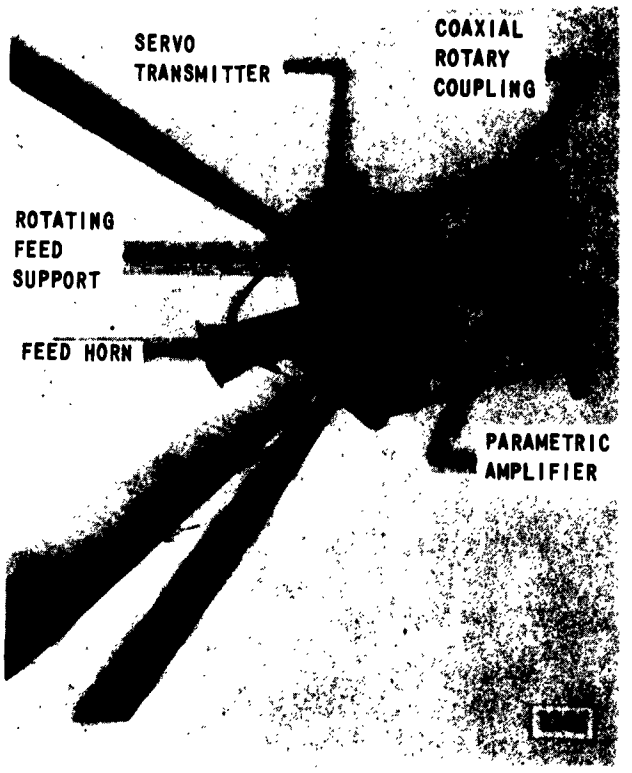

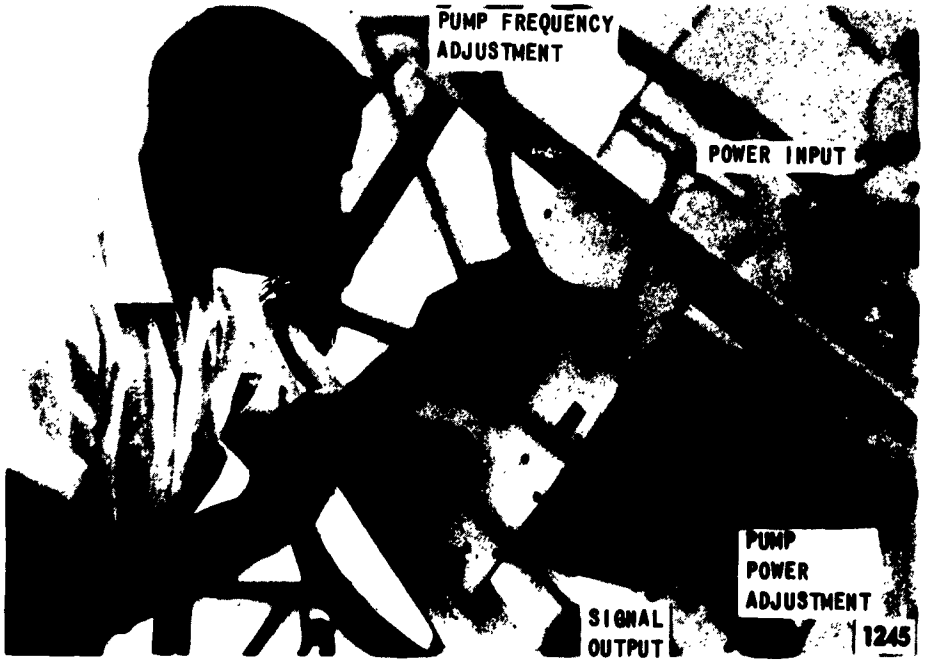

Figure 21 ANTENNA, FEED HORN, AND PARAMETRIC AMPLIFIER

There were five basic design goals for the receiver. Of primary importance to all experiments conducted was the receiver sensitivity, which is inversely related to the excess noise power generated by the receiving system. Thus, one of the most important parts of the receiver is a beam-type parametric amplifier,[1] a radio-frequency amplifier having a noise figure of less than 3 db, a gain of approximately 20 db, and a bandwidth, independent of gain, in excess of 40 mc. In operation the amplifier, in conjunction with a broad-band mixer and i-f amplifier, exhibits a double-channel noise figure of 1.5 db.[2] It is installed in a weatherproof housing and is mounted with the feed horn at the focus of the parabolic reflector (Figure 21).

The second design goal for the receiving system encompassed two mutually dependent requirements: high stability of frequency and very narrow bandwidth. These requirements were dictated by the nature of the lunar echo, which, as a consequence of the antennas in use and the radiated power level, appears at the output terminal of the receiving antenna as a signal of approximately -164 dbw. To enhance the signal-to-noise ratio of the received echo, the narrowest possible bandwidth was desirable. For the lunar echo at 915 mc, a bandwidth of 50 cps was found practical and adequate. This bandwidth requires a receiver frequency stability of approximately five parts in 10^8.

The required frequency stability is achieved through the use of a phase-locked reference generator[3] used in conjunction with a harmonic reference oscillator.[4] In operation, the oscillator generates a highly stable[5] signal at 1 mc. The basic 1-mc signal can be altered by ±25 cps, and any chosen frequency in this interval can be set to an accuracy of one part per thousand on a calibrated dial.

---

[1] Purchased from Zenith Radio Corporation.

[2] Appendix B for more information on the beam-type parametric amplifier.

[3] Manson model RD 170

[4] Manson model RD 110.

[5] Long-term stability: $1/10^8$ per day; short-term stability: $1/10^9$ Per minute.

The reference oscillator output was amplified and multiplied in the reference generator to obtain the 90th harmonic, which is used to phase lock a 90-mc, free-running oscillator. A further two-step multiplication results in the final output of 900 mc at a level of approximately 100 milliwatts, which is used as the local oscillator for the receiver. Because the frequency of the local oscillator is the 900th harmonic of the basic crystal frequency, the receiver may be tuned over an interval of $\pm$ 22.5 kc. This feature is not only desirable but necessary to compensate for the lunar Doppler shift from moonrise to moonset. Total frequency change is about 4 kc.

The required 50-cps bandwidth is achieved by use of a spectrum analyzer[1] in which the i-f bandwidth can be changed continuously from 10 cps to 20 kc. In this device, the sweep width is also continuously variable with a deviation of 0 cps to $\pm$ 50 kc. With the deviation set at zero, the spectrum analyzer acts like a variable bandwidth i-f amplifier and may be adjusted to the desired bandwidth of 50 cps.

During the experimental lunar echo program, it was soon determined that the lunar echo resembled band-limited noise in a near-unity ratio with a steady signal component. Because video spectrum analysis of such a signal will not only fold the radio frequency spectrum upon itself about the zero frequency line but will also be equal to a convolution of the spectrum we decided, as a third design goal, to incorporate a 200-cps i-f amplifier and to carry out spectrum analysis at that frequency. In the analog technique employed (Figure 22), the lunar echo is recorded on magnetic tape at the 200 cps i-f frequency. The tape speed during recording is 1-7/8 inches/second, and at that speed the bandwidth of the tape recorder is sufficient to preserve all the frequency components of the lunar echo. The tape containing real-time echo data at 1-7/8 inches/second is made into a closed belt and is subsequently played back at a speed of 60 inches/second into a spectrum analyzer having a resolution of 23 cps. Because the playback speed is stepped up 32 times over the record speed, each frequency component on the data tape is multiplied by 32 so that the original i-f frequency of 200 cps now appears as a frequency of 6.4 kc. Thus, the real-time resolution of this technique is 0.72 cps.

---

[1] Manufactured by Panoramic Products, Inc.

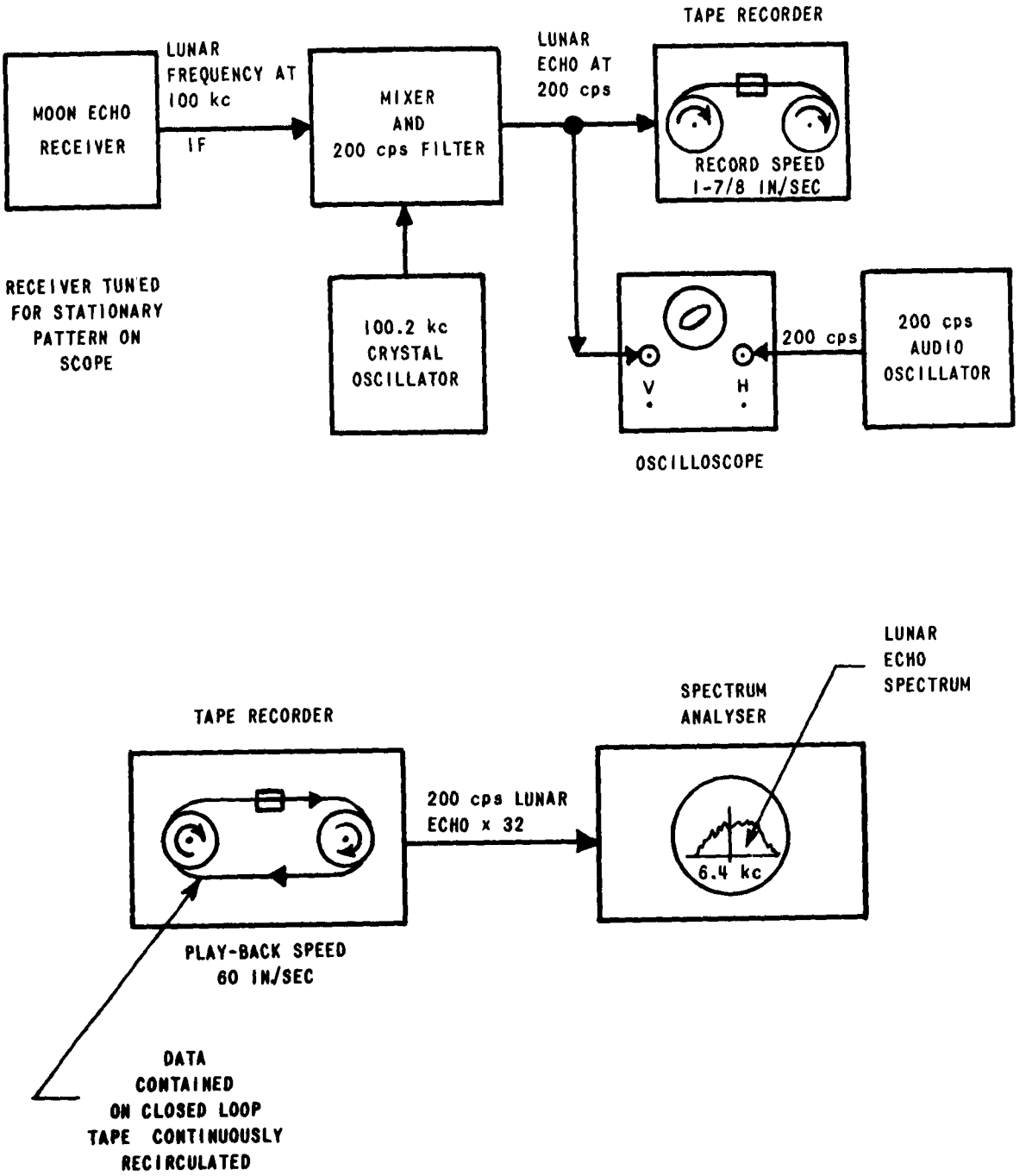

Figure 22 RECORDING SCHEME FOR LUNAR ECHO AT 200 cps I.F. AND DATA REDUCTION TECHNIQUE, BLOCK DIAGRAM

As far as the lunar experiment is concerned, the three design features of the receiver, consisting of high sensitivity, narrow bandwidth in conjunction with high frequency stability, and a low-frequency i-f amplifier, are sufficient to collect the required data. However, two additional receiver capabilities are required to carry out the auroral echo program and the radio star experiment, which will be reported separately. In particular, auroral echoes appear sporadically during auroral disturbances and are characterized by wide spectra (2 kc to 10 kc at the 3-db points) as well as positive or negative mean Doppler shifts. The auroral program, therefore, requires the receiver to monitor continuously a band of frequencies arranged ±15 kc about the transmission frequency of 915 mc. For this purpose, use is made of the spectrum-analyzer,[1] which for the lunar experiment acted merely as a narrow-band i-f amplifier. During the auroral experiment the spectrum analyzer sweeps a narrow i-f bandwidth filter ±5 kc about the center frequency, and the resulting video output is displayed as a function of deviation frequency on a cathode-ray oscilloscope. This display, which constitutes the spectrum of the auroral echo, is recorded photographically.

The final requirement for the receiver is the capability to act as a low-noise radiometer for the detection of extra-terrestrial radio sources. With the exception of the sun's radio emission, radio stars exhibit flux densities of less than 10^{-23} watts/cps-m^2 at 915 mc. For the receiver described thus far, the signal-to-noise ratio obtainable from even the strongest radio stars would be less than -10 db. However, this signal-to-noise ratio can be improved by integration of the signal to an extent proportional to $\sqrt{B\tau}$, where τ is the post-detection time constant and B is the predetection bandwidth. To obtain a desirable signal-to-noise ratio of 20 db, an improvement of 30 db is required; i.e. $B\tau \geq 10^6$. With a post-detection time constant of 1 second, the i-f bandwidth must be 1 mc. It will be observed in Figure 19 that the 15-mc preamplifier and i-f amplifier have a 4-mc bandwidth; referring next to Figure 23, it is evident that the peak detector time constant is 4.7 seconds. This combination of predetection bandwidth and post detection time constant results in a signal-to-noise improvement factor of 36.4 db.

---

[1] Panoramic Products, Inc.

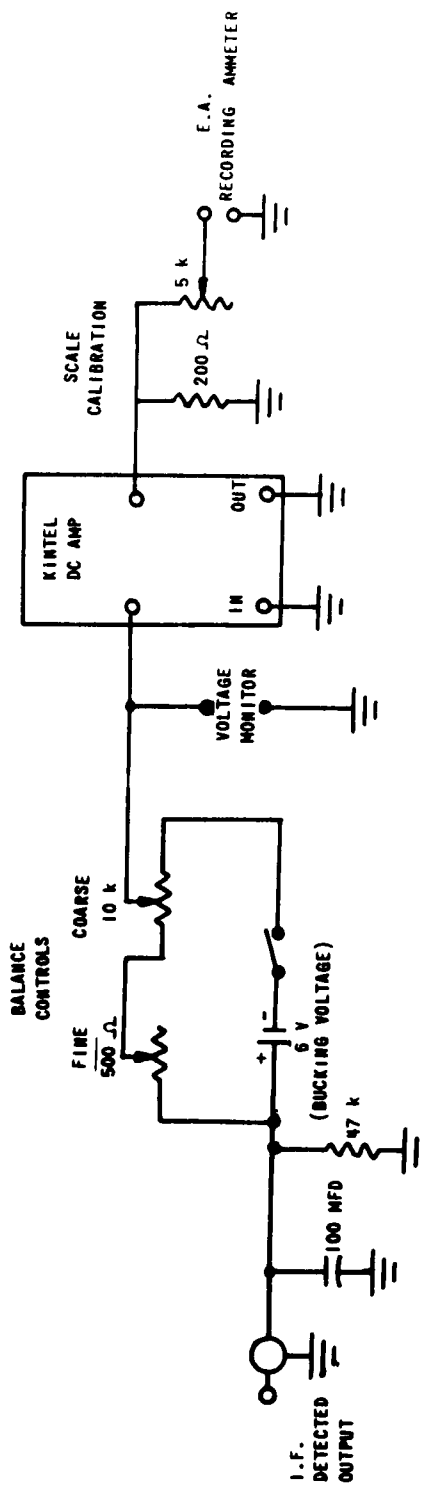

Figure 23 RADIO ASTRONOMY RECORDING SET-UP

Figure 23 also shows the technique employed to record the radio-star signals, and Figures 30 and 31 (Appendix C) show two resulting recordings. Connected in series with the peak detector output is an adjustable power supply arranged so as to oppose the average detected output from the 15-mc i-f amplifier. Consequently, the input voltage to the d-c amplifier is zero in the absence of a radio-star signal. In the presence of a radio-star signal, the small difference between the "bucking" voltage and the detected output is amplified and recorded on a pen recorder. [1]

Experimental data required for the lunar echo experiment consisted of signal polarization information, detected output from the 50-cps i-f amplifier, and the 200-cps i-f signal. The technique used for recording and processing the 200-cps i-f data has already been described. Outlined in Figure 24 is the digital recording scheme used to collect video data of the lunar echo. In that recording system, the 100-kc peak detector output is first converted to a frequency that is proportional to voltage. The average frequency during the gate time (0.1 sec) of the frequency counter is converted to a digital code and is transferred by the tape punch in standard teletype code on paper tape. With the particular frequency counter used here, a maximum sampling rate of 5 samples per second was possible. Transferring of the data collected on perforated tape to standard IBM cards and subsequent processing of these data were accomplished in the Laboratory's IBM 704 computer.

Polarization data of the lunar echo were recorded by the technique outlined in Figure 25. The 28-foot antenna in use at Newstead, New York, is equipped with a linearily polarized feed horn (Figure 21) which may be rotated either continuously or to any desired polarization by means of a reversible motor. A servo indicator of antenna polarization is incorporated on the antenna control panel. Coupled to the servo receiver is a linear potentiometer used in conjunction with a battery to provide an analog voltage of horn polarization. For data collection the feed horn is rotated continuously, and the analog polarization signal is recorded simultaneously with the detected output signal from the 915-mc receiver. Figure 26 shows a sample recording used for the determination of lunar echo polarization.

---

[1] Esterline Angus.

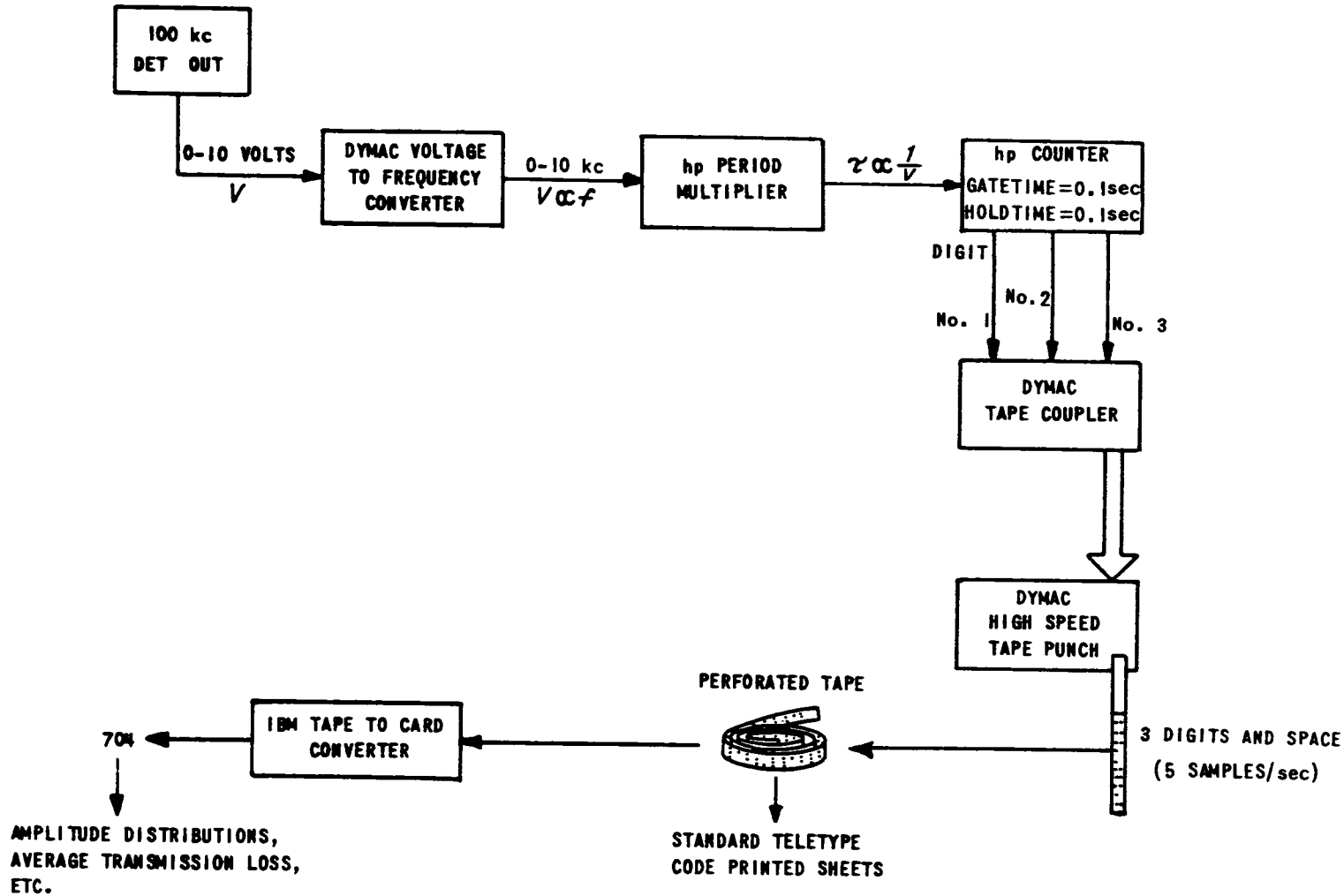

Figure 24 DIGITAL RECORDING SYSTEM

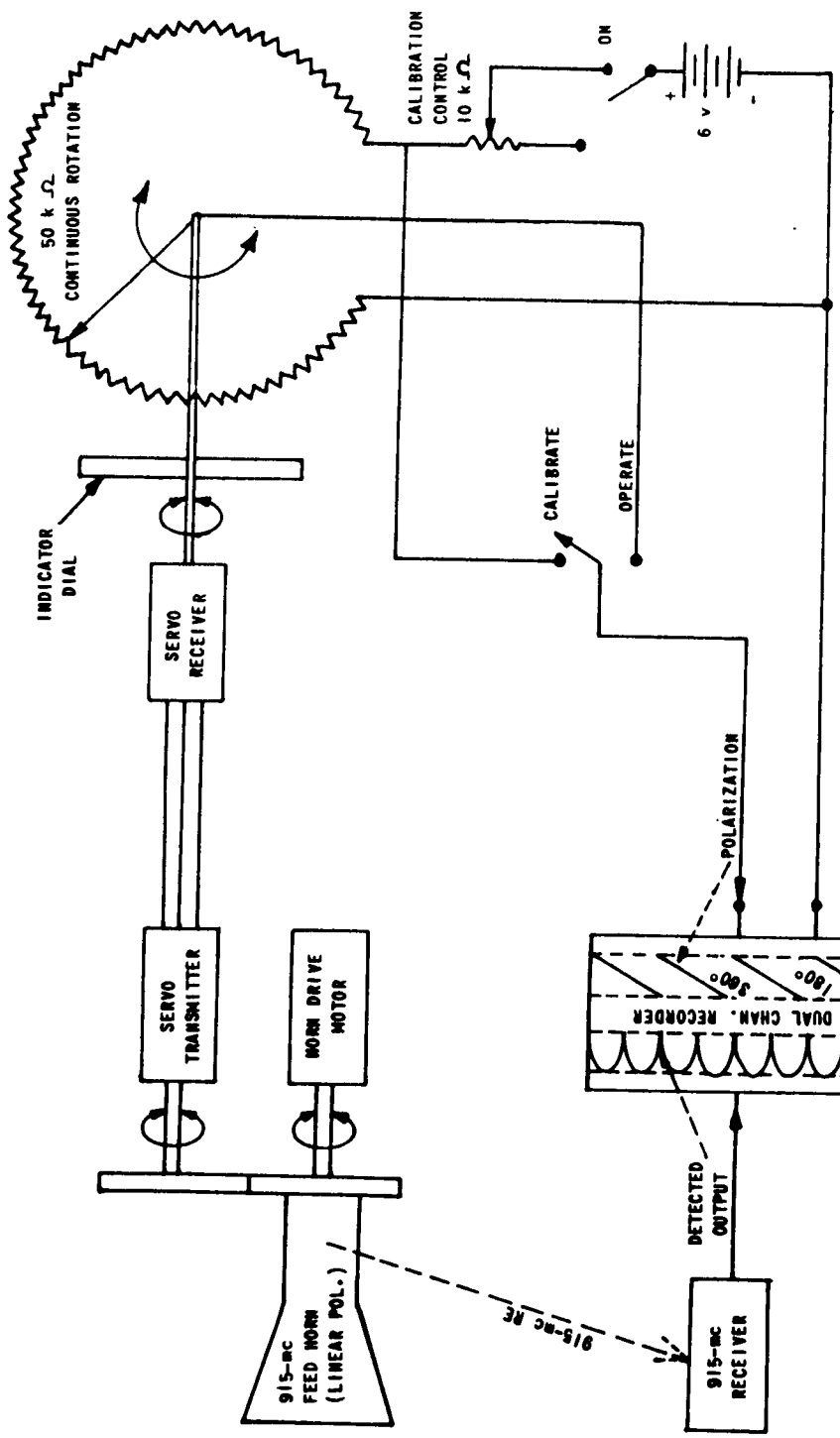

Figure 25 EXPERIMENTAL SET UP FOR POLARIZATION MEASUREMENTS

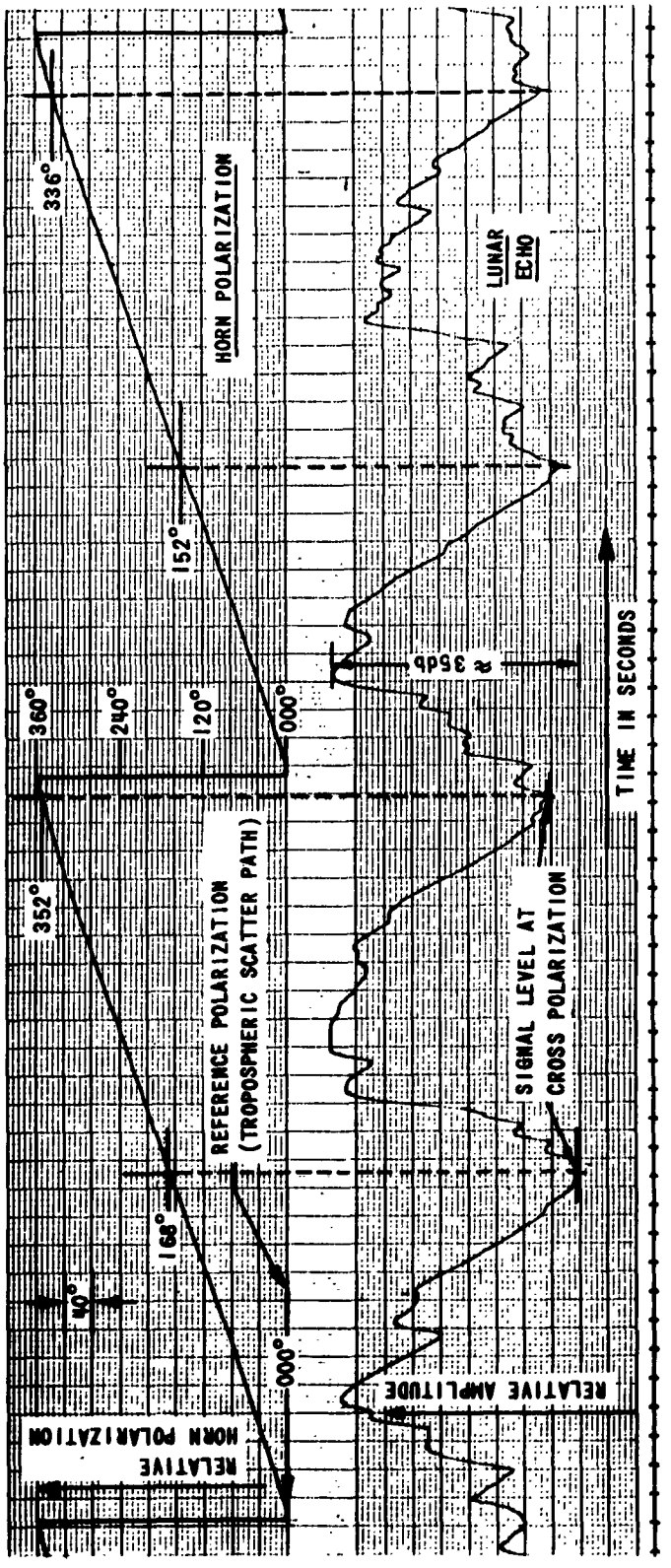

IPA79-1

Figure 26 SAMPLE RECORDING: DATA USED TO DETERMINE LUNAR ECHO POLARIZATION

Because determination of the average transmission loss over the Boston-Moon-Buffalo path was an important portion of the lunar echo program, the parameters of the 28-foot antenna at Newstead were determined experimentally. This experiment was carried out by recording the intensity of radio-star signals from Cassiopeia-A and Cygnus-A. The following antenna parameters were obtained:[1]

Effective aperture	45.35 meters^2 $\pm$ 3.75 meters^2
Antenna noise temperature:	48.8 °K $\pm$ 3.4 °K
Antenna noise power output per 50-cps bandwidth:	33.6 x 10^{-21} watts
Extra-galactic background temperature:	9 °K $\pm$ 3.4 °K
Half-power beamwidth:	3.42 degree

The sensitivity of the receiving system was computed from the receiver and antenna parameters. The double-channel noise figure of the receiver is 1.5 db, which represents an excess noise temperature of 124 °K. Thus, the single-channel excess noise temperature is 248 °K. To this figure must be added 115.6 °K, which comprises twice the sum of the sky noise and the antenna noise. On the basis of black-body radiation and the 28-foot antenna used, the moon contributes an effective increase of 0.139 °K in background temperature. Thus, in the determination of the noise level during lunar experiments, thermal radiation from the moon can be neglected. (Lunar thermal radiation can, however, be detected with the receiving equipment.) Consequently, the total effective excess noise temperature for the lunar experiment is 363.6 °K or an effective noise figure (single channel) of 3.5 db. In terms of total noise power output from the 50-cps i-f amplifier, this figure amounts to 2.5 x 10^{-19} watts or -186 dbw. Because it is unlikely that the antenna parameters will change with time, only periodic noise figure tests were conducted to assure that the noise level would remain constant.

---

[1] See Appendix C.

The input-output characteristics of the receiver are presented in Figures 27 and 28. The former figure shows the response of the receiving equipment at various i-f gain settings when the receiver is used as a radiometer. It will be observed, particularily at the low i-f gain settings, that the receiver response very nearly follows a square law. The characteristics shown in Figure 28 are applicable to the lunar- and auroral-echo experiments. This curve was obtained with the aid of a calibrated signal generator operated at an output level comparable to the lunar echo intensity. Typically during the lunar echo experiment, the average detected output from the 100-kc i-f amplifier was 2.5 to 3.0 volts.

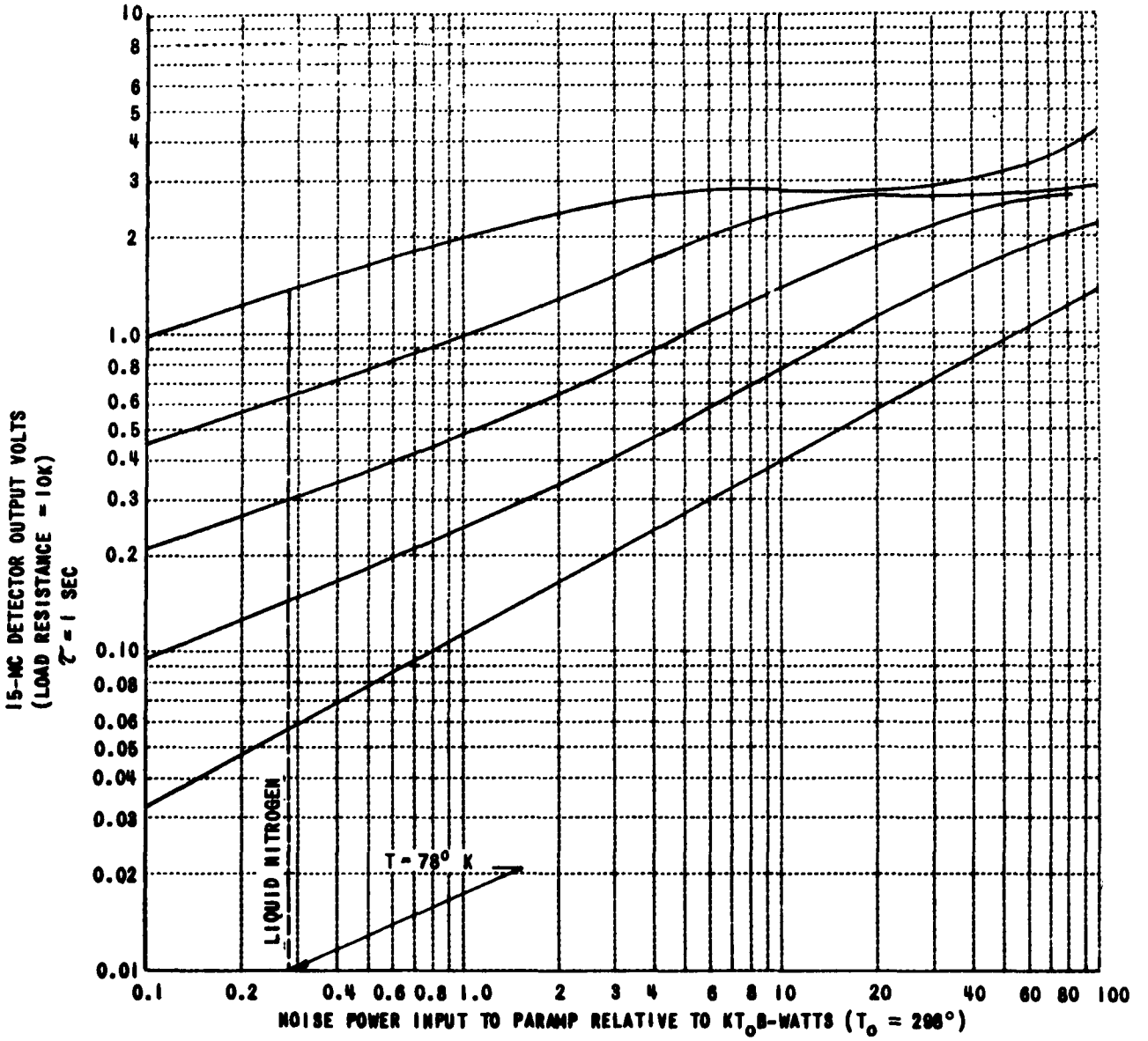

Figure 27 915-MC RECEIVER CHARACTERISTICS: 4-7-61

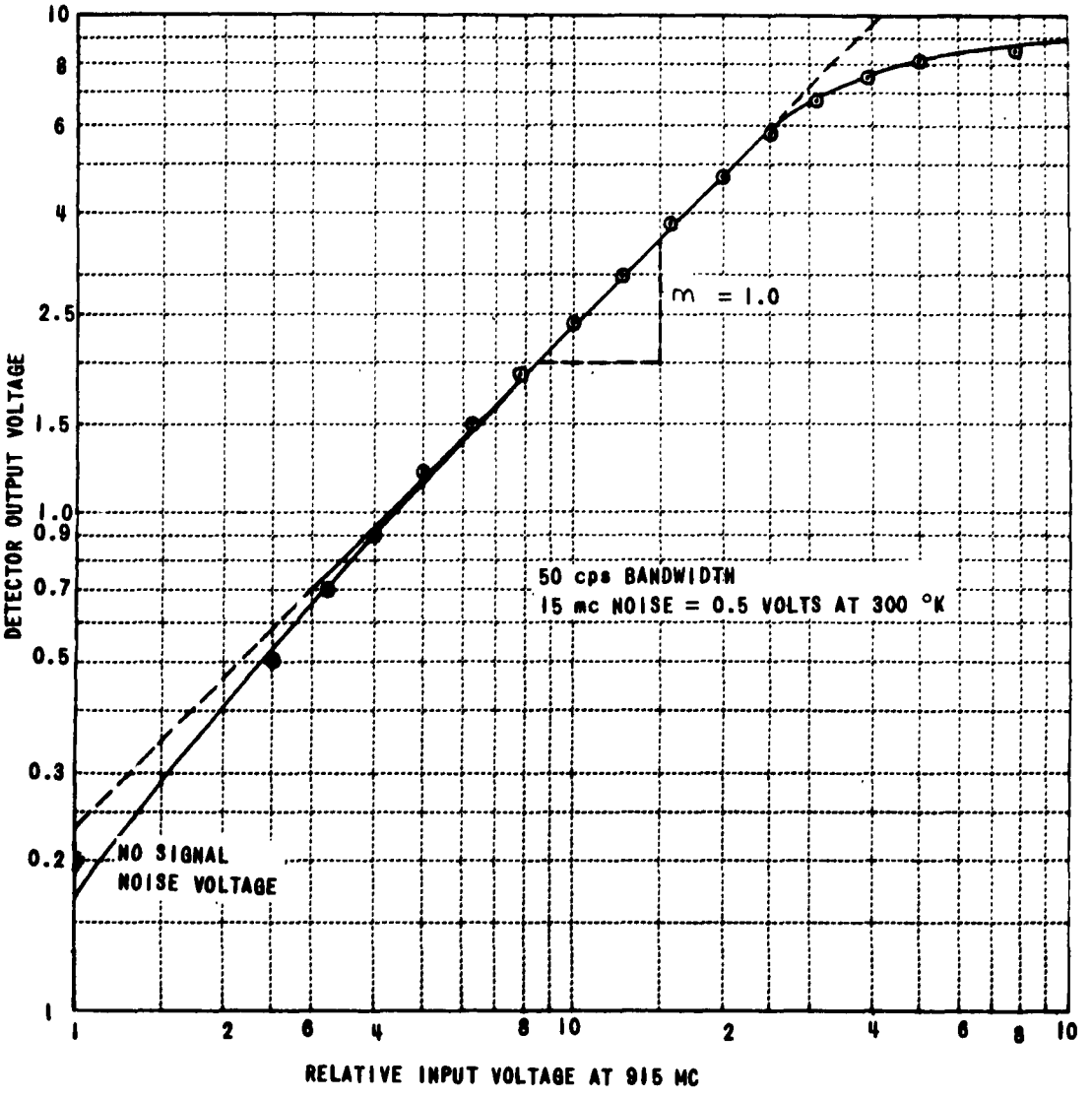

Figure 28 100-KC IF DETECTOR CHARACTERISTIC
RELATIVE INPUT VOLTAGE AT 915 MC

APPENDIX B

BEAM-TYPE PARAMETRIC AMPLIFIER

The beam-type parametric amplifier, or quadrapole amplifier, is a low-noise radio frequency amplifier developed by the Zenith Radio Corporation. Even though the parametric amplifying principle is used in this device, it differs from other parametric amplifiers primarily in that it utilizes an electron-beam tube rather than a solid-state varactor diode. In operation, the quadrapole amplifier exhibits a gain of approximately 20 db, independent of bandwidth, and a bandwidth in excess of 40 mc. The amplifier tube is "pumped" at a frequency equal to twice the signal frequency and thus is a degenerative device. Because of this degenerative feature, two different noise figures are realized depending upon whether the amplifier is used to amplify narrow-band signals or broad-band signals. The reason for this is best explained by examples.

Assume that the signal to be amplified consists of a single frequency. Two operations will be performed on this signal: it will be amplified, and it will be mixed with the pump frequency to produce the idler frequency. Because the pump frequency is twice the signal frequency, the resulting idler frequency is identical with the signal frequency. Consequently, the idler frequency will also be amplified so that it increases the useful output of the amplifier. At the same time, however, noise present in the idler channel, as well as in the signal channel, will deteriorate the sensitivity of the amplifier. Assume the magnitude of the noise power in each channel to be N watts. Then the total noise output of the amplifier is $2NG$ watts, where G is the amplifier gain. Likewise, since the idler channel coincides with the signal channel, twice the signal power (times the gain) appears at the output. Consequently, under the circumstances described (synchronous pumping) the presence of the idler channel may be neglected.

Assume next that there is a finite frequency difference (Δf) between the idler frequency and the signal frequency. As before, noise power enters both channels, but, in comparison with the synchronous pumping case the idler

frequency vector now rotates with respect to the signal frequency vector at a rate equal to $\Delta\omega$. It will be seen that the resulting output from the amplifier consists of the vector sum of the signal voltage and the idler voltage. The rms value of the noise power output is still the same as in the previous case, but useful power output has been reduced.

Suppose for a third condition that the idler frequency and the signal frequency are separated by an amount (Δf), which is larger than the narrowest bandwidth of the entire receiving system. Under these circumstances, only the signal channel can be utilized, but noise enters both the signal and the idler channel. This is the worst condition possible (as far as noise figure is concerned) and is referred to as single-channel operation. It is easy to see that, in comparison with synchronous pumping (or double-channel operation), the noise figure for single-channel operation has doubled.

Even though the noise figure is not as good for single-channel operation as it is for double-channel operation, single-channel operation has one great advantage. Because only the signal channel is preserved and amplified, amplitude as well as phase information is preserved during this mode of operation. All phase information contained in the original signal is lost in the first two situations because the quadrature components of the signal vector and idler vector cancel. This phenomenon is not a disadvantage under circumstances in which phase information is unimportant. One specific application of the double channel mode is in radio astronomy where the signal to be amplified is randomly phased and has a very broad frequency spectrum; synchronous pumping requirements are automatically satisfied for any given i-f bandwidth.

For a more complete description of the theoretical aspects of the quadrapole amplifier reference is made to an article by Robert Adler et al., "The Quadrapole Amplifier, a Low-Noise Parametric Device," Proc. IRE, 47, 10, pp. 1713-1723 (1959).

APPENDIX C

CALIBRATION OF 28-FOOT ANTENNA SYSTEM WITH NOISE SOURCES

A. Theory

An antenna, which collects all of the power from a noise source of KT_1B watts, will deliver an output power $N_1 = FKTB$ watts, where F is the "figure of merit" for the antenna.[1] Consequently, the noise power generated by the antenna is $N_0 = KT_1B(F-1)$ watts (which, of course, is zero for $F=1$). If the antenna collects power from a second noise source, the output power will be $N_2 = FKT_2B$ watts. However, only KT_2B watts were originally collected and $KT_1B(F-1)$ watts were introduced by the antenna. Therefore,

$$N_2 = KT_2B + N_0 \text{ watts}$$

or $$N_2 = KT_2B + N_1 - KT_1B \text{ watts}$$

Then: $$N_2 - N_1 = KB(T_2 - T_1)$$

But $N_1 = FKBT_1$ or $KB = \frac{N_1}{FT_1}$, which when substituted will give

$$\frac{N_2}{N_1} - 1 = \left\{\frac{T_2}{T_1} - 1\right\}\frac{1}{F}$$

or $$F = \frac{\left[\frac{T_2}{T_1} - 1\right]}{\left[\frac{N_2}{N_1} - 1\right]}$$

---

[1] K = Boltzman's constant. (1.38×10^{-23} joules/degree K
T = temperature in degrees K
B = bandwidth in cps.

If now two noise sources are available, such as two "radio stars," the fluxes S_i of which are given in terms of watts/m^2 - cps, then equivalent noise temperatures can be computed by $KT_iB = S_iAB$ where A is the collecting area of the antenna. Consequently, $T = \frac{SA}{K}$, and $\frac{T_2}{T_1} = \frac{S_2}{S_1}$. If now the ratio of output powers from the antenna is known, F can be computed without a knowledge of the antenna area. Knowing the figure of merit for the antenna, we can compute the area of the antenna from the relation

$$\frac{N_1}{F} = KT_1B = S_1A$$

or

$$A = \frac{N_1}{S_1F} \text{ meters}^2$$

Knowing the antenna aperture, we can solve for the antenna noise temperature from the relation

$$N_0 = KT_0B = KT_1B(F-1)$$

or

$$T_0 = \frac{S_1A}{K}(F-1)\ ^\circ K.$$

B. Experimental Procedure

The antenna to be calibrated is a 28-foot parabola operated at 915 mc. The detected output from the receiver is calibrated in terms of input noise power (Figure 29). Thus, $(V_{out})^{2.5} = CP_{in}$. At $\lambda = 0.328$ meters ($f = 915$ mc), the following radio-star fluxes are assumed:

Cassiopeia A : $S_1 = 21.9 \times 10^{-24}$ watts/m^2 - cps
Cygnus A : $S_2 = 16.2 \times 10^{-24}$ watts/m^2 - cps

Then:

$$\frac{T_2}{T_1} = \frac{S_2}{S_1} = \frac{21.9}{16.2} = 1.352$$

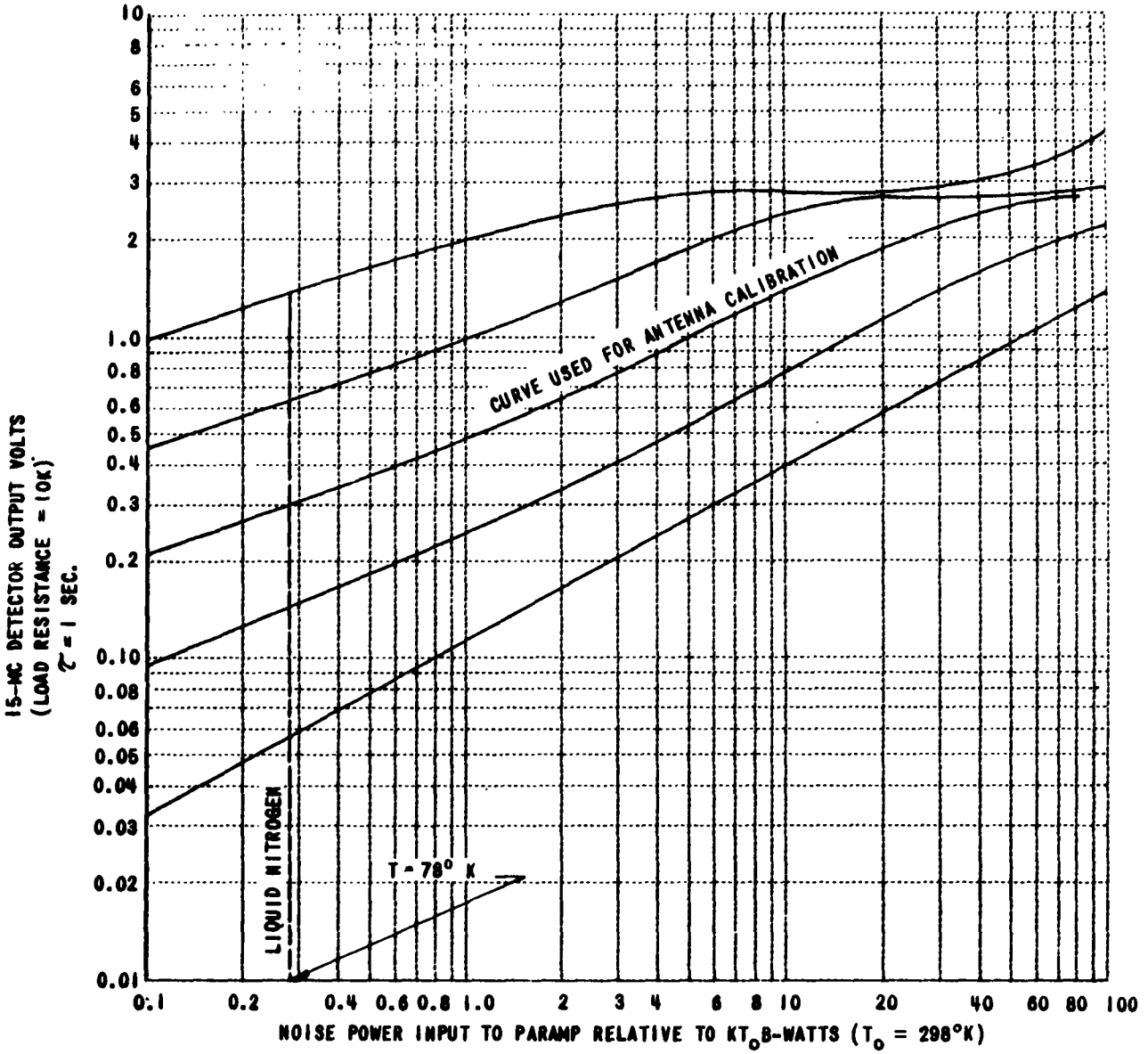

Figure 29 915-MC RECEIVER CHARACTERISTICS: 4-7-61

The output voltages recorded were 0.283 volts for Cygnus (Figure 30) and 0.299 volts for Cassiopeia (Figure 31).

Consequently $$\frac{N_2}{N_1} = \left(\frac{.299}{.283}\right)^{2.5} = 1.15$$

Then: $$F = \frac{1.352 - 1}{1.15 - 1} = \frac{.352}{.15} = 2.34$$

Since the actual antenna in use is linearly polarized, and the radio-star signal is randomly polarized, the amount of power actually received is one-half of the incident power. Consequently,

$$S_1' = 10.95 \times 10^{-24} \text{ watts/m}^2\text{-cps}$$

Because 0.300 is the receiver voltage output for an input of 78°K, the actual power received was $\left(\frac{.299}{.300}\right)^{2.5} 78°\text{KB}$ watts.

Then: $$A = \frac{77.5\ KB}{(2.34)(10.95)(10^{-24})B} = \frac{(77.5)(13.8)}{(2.34)(10.95)} = \underline{\underline{41.6\ m^2}}$$

Likewise for Cygnus A, $S_2' = 8.1 \times 10^{-24}$ watts/m^2 cps and the actual received power was $\left(\frac{.283}{.300}\right)^{2.5} 78$ KB = 67.5 KB watts

and $$A = \frac{(67.5)(13.8)}{(2.34)(8.1)} = 49.1 \text{ meter}^2$$

Solving next for T_o

$$T_o = \frac{10.95}{13.8}(1.34)A$$

$$\left.\begin{aligned} T_o &= 45.3°K \\ \text{or} \quad &= 52.2°K \end{aligned}\right\} \text{depending on choice of source brightness}$$

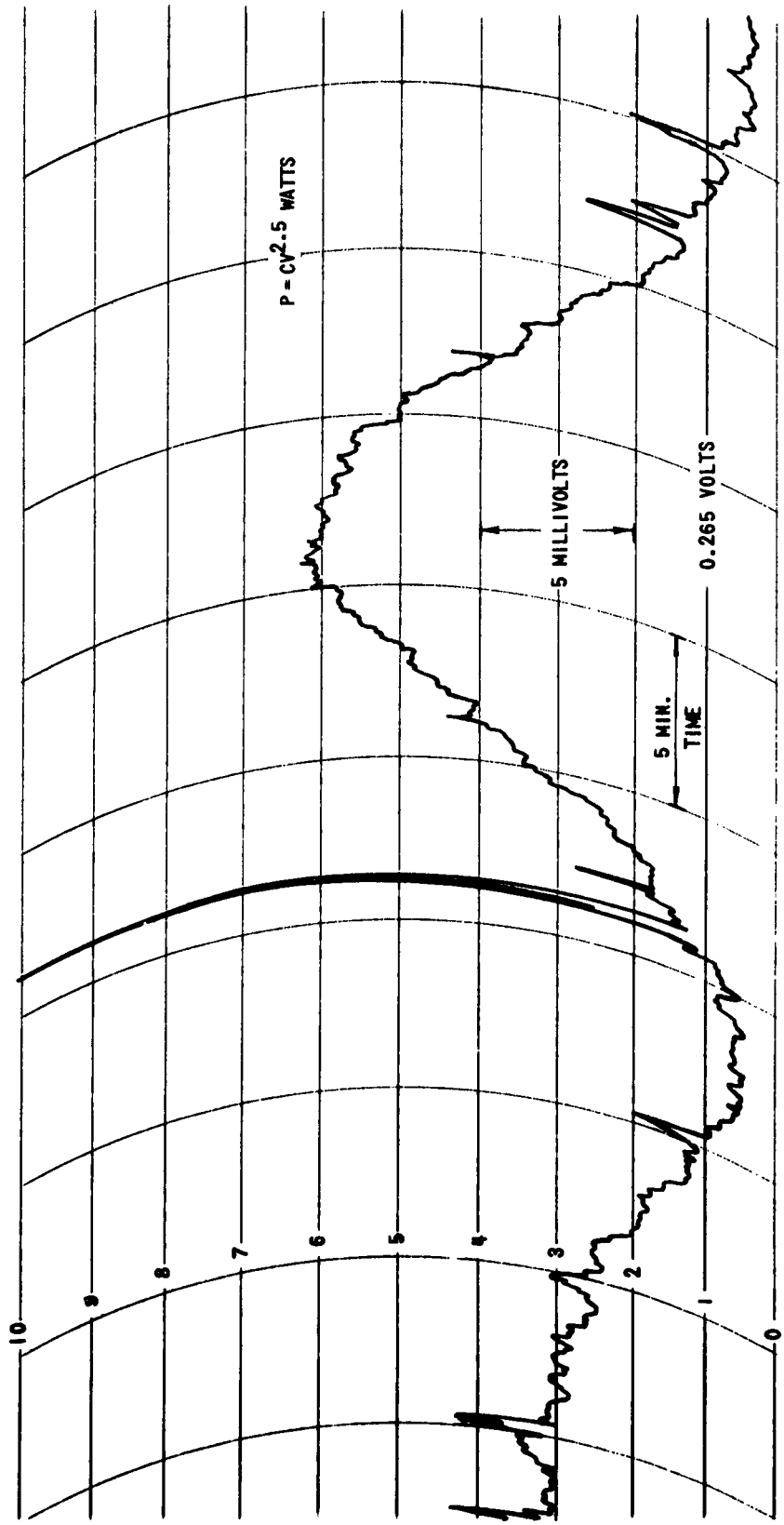

Figure 30 CYGNUS-A DRIFT PATTERN (4-11-61 - 1030 EST)

Figure 31 CASSIOPEIA-A DRIFT PATTERN (4-11-61 - 1805 EST)

The error here is ±7 percent in area with a consequent uncertainty of T_o of ±3.4°K. Assuming now an average T_o of 48.8°K, we can deduce the background, or sky temperature, to be T_S so that

$$N_S = KT_S B + KT_o B$$

or $$\left(\frac{.266}{.300}\right)^{2.5} 78° = T_S + T_o = 57.8°$$

or $$T_S = 57.8 - 48.8 = 9°K \pm 3.4°K$$

Assume that the average antenna area is

$$A = 45.35\, m^2 = \frac{\pi D^2}{4}$$

where D is the effective diameter of the antenna,

and $$D = 6.73 \text{ meters} = 22 \text{ feet}$$

Then, the half-power beam angle is θ so that

$$\theta = \frac{70\lambda}{D} = 3.42°$$

The predicted half-power beamwidth of 2.6° = θ .

APPENDIX D

COMPUTATION OF MOON DOPPLER MAP

1. INTRODUCTION

An experiment to measure the electromagnetic-reflection characteristics of the moon was carried out by the Cornell Aeronautical Laboratory during 1959 through 1961. A crystal-controlled 915-mc c-w signal was relayed to a receiver at the Laboratory from a transmitter located at Bedford, Massachusetts, by means of reflection from the moon; the characteristics of the received signal were then measured and recorded.

One prominent characteristic noted in the experiment was a fading of the received signal -- a phenomenon due in part to the "beating" together of signals received from different parts of the moon. The beats arise from relative differences in the velocities of the parts of the moon's surface for which reflections toward the receiver occur, resulting in varying Doppler shifts in the frequency of the reflected signals. That is, the frequency of a signal reflected from one edge of the moon may differ from that reflected from the center by as much as twenty cycles in a billion, owing to the relative motion of these two parts of the moon's surface, as seen from the earth. The purpose of this Appendix is to outline the method used to compute the Doppler shift for selected points on the surface of the moon.

2. THE DOPPLER EFFECT

Consider a frame of reference Σ' moving with velocity $\vec{V}$ with respect to another frame of reference Σ. Electromagnetic radiation observed to have frequency ω' in Σ will be observed to have a frequency

$$\omega = \omega' \frac{1 + \left|\frac{\vec{V}}{c}\right| \cos\alpha'}{\sqrt{1 - \left(\frac{V}{c}\right)^2}} \qquad (1)$$

in Σ,

where α' is the angle between $\vec{V}$ and the direction in which the radiation is propagated in Σ, so that it reaches the observer in Σ.

This same angle observed in Σ is given by

$$\cos\alpha = \frac{\cos\alpha' + \beta}{1 + \beta\cos\alpha} \tag{2}$$

where $\beta = |\vec{V}|/c$.

Thus, the frequency observed in Σ in terms of the angle of propagation observed in Σ is

$$\omega = \omega' \frac{\sqrt{1-\beta^2}}{1-\beta\cos\alpha} \tag{3}$$

3. POSITIONS AND VELOCITIES ON THE EARTH AND MOON

In order that the shift in observed frequency between Bedford and Buffalo may be calculated, the positions and velocities of these two points, as well as those of the chosen reflection point on the moon must be specified.

A. On the Earth

Position on the earth will be specified by right ascension (absolute longitude) from the true equinox and declination (latitude) from the equator. Thus, the right ascension of Buffalo at any time is given by the relation

$$\text{(R.A. of Buffalo)} = \text{(Longitude of Buffalo)} + \text{(Rate of earth's rotation)}\ (t - t_{\text{equinox}})$$

where t_{equinox} is the time of the vernal equinox, and the rate of the earth's rotation is measured with respect to the true equinox, which is defined to be the intersection of the plane of the ecliptic with the earth's equatorial plane. Universal time, which is mean solar time measured from midnight, will be used throughout.

If the true equinox is defined as the X axis of an "inertial" reference system, with the earth's spin axis as the Z axis, the X, Y, and Z components of the radius vector from the center of the earth to a point on the surface may be written as:

$$\begin{aligned} X^e &= R_e \cos \varphi_e^E \cos \Phi_e^E \\ Y^e &= R_e \sin \varphi_e^E \cos \Phi_e^E \\ Z^e &= R_e \sin \Phi_e^E \end{aligned} \tag{4}$$

where R_e = the radial distance to the point e

φ_e^E = the right ascension of the point e, and

Φ_e^E = the declination (latitude) of the point e.

B. Matrix Representation

The angles φ_e^E and Φ_e^E may also be considered as defining the rotations necessary to align the X axis with the vector $\vec{R}_e$. These rotations then define a new coordinate system, say X_1, Y_1, Z_1 in which the components of $\vec{R}_e$ are $X_1^e = R_e$ and $Y_1^e = Z_1^e = 0$. These two rotations may be expressed as matrices multiplying the X, Y, Z coordinates as follows:

$$\begin{pmatrix} X_1 \\ Y_1 \\ Z_1 \end{pmatrix} = \begin{pmatrix} \cos \Phi_e^E & 0 & \sin \Phi_e^E \\ 0 & 1 & 0 \\ -\sin \Phi_e^E & 0 & \cos \Phi_e^E \end{pmatrix} \begin{pmatrix} \cos \varphi_e^E & \sin \varphi_e^E & 0 \\ -\sin \varphi_e^E & \cos \varphi_e^E & 0 \\ 0 & 0 & 1 \end{pmatrix} \begin{pmatrix} X \\ Y \\ Z \end{pmatrix} \tag{5}$$

If the indicated multiplication is performed, the matrices will give the result stated above. Calling the Φ rotation matrix $T_{\Phi_e^E}$ and the φ-rotation matrix $T_{\varphi_e^E}$, Equation 5 may be rewritten as

$$\begin{pmatrix} X_1 \\ Y_1 \\ Z_1 \end{pmatrix} = T_{\Theta_e^\varepsilon}\ T_{\varphi_e^\varepsilon} \begin{pmatrix} X \\ Y \\ Z \end{pmatrix} \tag{6}$$

To get the X , Y , Z coordinates of a point from its X_1 , Y_1 , Z_1 coordinates, the X axis must be rotated back to its original position. This rotation is accomplished by two matrices which are the <u>inverses</u> of the first two:

$$\begin{pmatrix} X \\ Y \\ Z \end{pmatrix} = T_{\varphi_e^\varepsilon}^{-1}\ T_{\Theta_e^\varepsilon}^{-1} \begin{pmatrix} X_1 \\ Y_1 \\ Z_1 \end{pmatrix} \tag{7}$$

where

$$T_{\varphi_e^\varepsilon}^{-1} = \begin{pmatrix} \cos\varphi_e^\varepsilon & -\sin\varphi_e & 0 \\ \sin\varphi_e^\varepsilon & \cos\varphi_e^\varepsilon & 0 \\ 0 & 0 & 1 \end{pmatrix}$$

$$T_{\Theta_e^\varepsilon}^{-1} = \begin{pmatrix} \cos\Theta_e^\varepsilon & 0 & -\sin\Theta_e^\varepsilon \\ 0 & 1 & 0 \\ \sin\Theta_e^\varepsilon & 0 & \cos\Theta_e^\varepsilon \end{pmatrix}$$

Notice that the matrices are applied in <u>reverse</u> order to the X_1 , Y_1 , Z_1 coordinates. Now putting $X_1 = R_e$, $Y_1 = 0$ we obtain

$$\begin{pmatrix} X^e \\ Y^e \\ Z^e \end{pmatrix} = T_{\psi_e^\varepsilon}^{-1} \; T_{\theta_e^\varepsilon}^{-1} \begin{pmatrix} R \\ 0 \\ 0 \end{pmatrix} \tag{8}$$

which, when multiplied out, yields Equation 4 once again.

To obtain the X , Y , and Z components of the velocity of the point e , the above expression is differentiated with respect to time, with the result

$$\begin{pmatrix} \dot{X}^e \\ \dot{Y}^e \\ \dot{Z}^e \end{pmatrix} = \frac{\partial T_{\psi_e^\varepsilon}^{-1}}{\partial \psi_e^\varepsilon} \; T_{\theta_e^\varepsilon}^{-1} \begin{pmatrix} R_e \\ 0 \\ 0 \end{pmatrix} \dot{\psi}_e^\varepsilon \tag{9}$$

where $\left(\partial T_{\psi_e^\varepsilon}^{-1} / \partial \psi_e^\varepsilon\right)$ is just the derivative of each element of the matrix with respect to ψ_e^ε .

C. On the Moon

The position of a point on the moon will be specified by its selenographic latitude and longitude -- that is, the latitude and longitude as measured from a coordinate system fixed at the center of the moon, with its X axis passing through the mean center of the moon's visible disk, and its Z axis pointing along the spin axis of the moon. To obtain the X , Y , and Z coordinates of any point, it will be necessary to specify the location of the moon's center and the orientation of the selenographic coordinate system with respect to the X , Y , Z system.

The position of the moon's center will be specified by its right ascension and declination, as discussed before, and by the length of the radius vector from the center of the earth, which will be obtained from the angle

subtended at the center of the moon by the equatorial radius of the earth, known as the horizontal parallax. The length of this vector is given by the relation

$$R_m = \frac{6,378,388}{\sin(H.P.)} \quad meters$$

Using the matrix notation discussed above, the X , Y , Z components of the radius vector to the moon may be written as

$$\begin{pmatrix} X^m \\ Y^m \\ Z^m \end{pmatrix} = T_{\varphi_m^\epsilon}^{-1} \; T_{\Phi_m^\epsilon}^{-1} \begin{pmatrix} R_m \\ 0 \\ 0 \end{pmatrix} \tag{10}$$

where φ_m^ϵ is the right ascension of the moon and Φ_m^ϵ is its declination.

The orientation of the selenographic coordinate system with respect to the X , Y , Z system will be specified by the angle of inclination of the moon's equator to the earth's equator (β), the angle between the true equinox and the intersection of these two equators (α), and the angle between this intersection and the selenographic X axis (γ).

The location of a point on the moon will be specified, as previously stated, by its selenographic latitude (Φ_p^m) and longitude (φ_p^m).

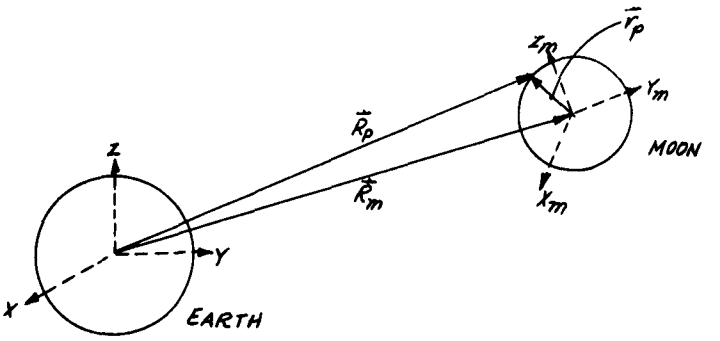

As can be seen from the diagram above, the vector $\vec{R}_p$ from the center of the earth to a point p on the surface of the moon can be written as the sum of two vectors: $\vec{R}_m$ from the center of the earth to the center of the moon, and $\vec{r}_p$ from the center of the moon to the point p. To obtain the X, Y, Z components of $\vec{R}_p$, it is necessary to find the X, Y, Z components of and add these to the components of $\vec{R}_m$ given above.

The X^m, Y^m, Z^m components of $\vec{r}_p$ may be written in matrix notation as

$$\begin{pmatrix} X_p^m \\ Y_p^m \\ Z_p^m \end{pmatrix} = T_{\varphi_p^m}^{-1} \; T_{\Phi_p^m}^{-1} \begin{pmatrix} r_p \\ 0 \\ 0 \end{pmatrix} \tag{11}$$

where

$$T_{\varphi_p^m}^{-1} = \begin{pmatrix} \cos\varphi_p^m & -\sin\varphi_p^m & 0 \\ \sin\varphi_p^m & \cos\varphi_p^m & 0 \\ 0 & 0 & 1 \end{pmatrix}$$

$$T_{\Phi_p^m}^{-1} = \begin{pmatrix} \cos\Phi_p^m & 0 & -\sin\Phi_p^m \\ 0 & 1 & 0 \\ \sin\Phi_p^m & 0 & \cos\Phi_p^m \end{pmatrix} \tag{12}$$

To obtain the X, Y, Z components of $\vec{r}_p$, the X^m, Y^m, Z^m system must be rotated to coincide with X, Y, Z. This can be done by rotating on the angles α, β, γ defining the orientation of X^m, Y^m, Z^m. In matrix notation, these rotations are

$$T_\alpha^{-1} = \begin{pmatrix} \cos\alpha & -\sin\alpha & 0 \\ \sin\alpha & \cos\alpha & 0 \\ 0 & 0 & 1 \end{pmatrix}$$

$$T_\beta^{-1} = \begin{pmatrix} 1 & 0 & 0 \\ 0 & \cos\beta & -\sin\beta \\ 0 & \sin\beta & \cos\beta \end{pmatrix} \qquad (13)$$

$$T_\gamma^{-1} = \begin{pmatrix} \cos\gamma & -\sin\gamma & 0 \\ \sin\gamma & \cos\gamma & 0 \\ 0 & 0 & 1 \end{pmatrix}$$

The X , Y , Z components of $\vec{r}_p$ are given by

$$\begin{pmatrix} X \\ Y \\ Z \end{pmatrix} = T_\alpha^{-1}\, T_\beta^{-1}\, T_\gamma^{-1} \begin{pmatrix} X^m \\ Y^m \\ Z^m \end{pmatrix}$$

$$= T_\alpha^{-1} T_\beta^{-1} T_\gamma^{-1} T_{y_p}^{-1m}\, T_{\circledcirc_p}^{-1m} \begin{pmatrix} r_p \\ 0 \\ 0 \end{pmatrix} \qquad (14)$$

Thus, the X , Y , Z components of $\vec{R}_p$ are given by

$$\begin{pmatrix} X^p \\ Y^p \\ Z^p \end{pmatrix} = T_{y_m}^{-1\varepsilon}\, T_{\circledcirc_m}^{-1\varepsilon} \begin{pmatrix} R_m \\ 0 \\ 0 \end{pmatrix} + T_\alpha^{-1} T_\beta^{-1} T_\gamma^{-1} T_{y_p}^{-1m}\, T_{\circledcirc_p}^{-1m} \begin{pmatrix} r_p \\ 0 \\ 0 \end{pmatrix} \qquad (15)$$

D. Velocity of the Point on the Moon

The X , Y and Z components of the velocity of the point $\vec{R}_p$ are found by differentiating the expression obtained above term by term:

$$\begin{pmatrix} \dot{X}^p \\ \dot{Y}^p \\ \dot{Z}^p \end{pmatrix} = \dot{\vec{R}}_m + \dot{\vec{r}}_p =$$

$$\frac{\partial T^{-1}_{\psi^E_m}}{\partial \psi^E_m} T^{-1}_{\Phi^E_m} \begin{pmatrix} R_m \\ 0 \\ 0 \end{pmatrix} \dot{\psi}^E_m + T^{-1}_{\psi^E_m} \frac{\partial T^{-1}_{\Phi^E_m}}{\partial \Phi^E_m} \begin{pmatrix} R_m \\ 0 \\ 0 \end{pmatrix} \dot{\Phi}^E_m +$$

$$T^{-1}_{\psi^E_m} T^{-1}_{\Phi^E_m} \begin{pmatrix} \dot{R}_m \\ 0 \\ 0 \end{pmatrix} + \frac{\partial T^{-1}_\alpha}{\partial \alpha} T^{-1}_\beta T^{-1}_\gamma T^{-1}_{\psi^m_p} T^{-1}_{\Phi^m_p} \begin{pmatrix} r_p \\ 0 \\ 0 \end{pmatrix} \dot{\alpha} + \tag{16}$$

$$T^{-1}_\alpha \frac{\partial T^{-1}_\beta}{\partial \beta} T^{-1}_\gamma T^{-1}_{\psi^m_p} T^{-1}_{\Phi^m_p} \begin{pmatrix} r_p \\ 0 \\ 0 \end{pmatrix} \dot{\beta} + T^{-1}_\alpha T^{-1}_\beta T^{-1}_\beta \frac{\partial T^{-1}_\gamma}{\partial \gamma} T^{-1}_{\psi^m_p} T^{-1}_{\Phi^m_p} \begin{pmatrix} r_p \\ 0 \\ 0 \end{pmatrix} \dot{\gamma} +$$

$$T^{-1}_\alpha T^{-1}_\beta T^{-1}_\gamma \frac{\partial T^{-1}_{\psi^m_p}}{\partial \psi^m_p} T^{-1}_{\Phi^m_p} \begin{pmatrix} r_p \\ 0 \\ 0 \end{pmatrix} \dot{\psi}^m_p + T^{-1}_\alpha T^{-1}_\beta T^{-1}_\gamma T^{-1}_{\psi^m_p} \frac{\partial T^{-1}_{\Phi^m_p}}{\partial \Phi^m_p} \begin{pmatrix} r_p \\ 0 \\ 0 \end{pmatrix} \dot{\Phi}^m_p$$

Note that $\dot{\psi}^m_p$ and $\dot{\Phi}^m_p$ are the rates of change of position of a point on the moon's surface within the moon's own coordinate system. These are called the physical libration rates and amount to only 0.001 degree per day. Calculation of the contributions of these terms to the Doppler shift will be made to determine if they are, as suspected, negligible.

4. THE ANGLES OF PROPAGATION

To circumvent the problem of determining the angles of propagation observed in the reference frames at Bedford, Buffalo, and on the moon, all angles will be referred to the "inertial" system X, Y, Z defined previously.

Thus, a frequency ω_0 broadcast from Bedford will appear, to an observer situated on the line connecting the instantaneous position of Bedford with the point in space where reflection at the moon will take place, to be

$$\omega_1 = \frac{\omega_0 \sqrt{1-\beta_e^2}}{1-\beta_e \cos\alpha_1} \tag{17}$$

where β_e is the magnitude of the velocity of the point e divided by the velocity of light c, and α_1 is the angle in the x, y, z system between this velocity vector and the line passing through the observer's position.

The frequency ω_2 which will be observed on the moon at point p is similarly related to ω_1 by

$$\omega_1 = \frac{\omega_2 \sqrt{1-\beta_p^2}}{1-\beta_p \cos\alpha_2} \tag{18}$$

where β_p is the magnitude of $\vec{V}_p$ divided by c, and α_2 is the angle between $\vec{V}_p$ and the line passing through the stationary observer's position.

On the return leg of the trip from the moon to Buffalo, the radiation is propagated in the opposite direction. Thus, the frequency observed in transit to earth is given by

$$\omega_3 = \frac{\omega_2 \sqrt{1-\beta_p^2}}{1-\beta_p \cos\alpha_3} \tag{19}$$

where α_3 is the angle between $\vec{V}_p$ and the line connecting the point of reflection to the receiving station at Buffalo.

Finally, the frequency ω_4 observed at Buffalo is related to ω_3 by

$$\omega_3 = \frac{\omega_4 \sqrt{1-\beta_f^2}}{1-\beta_f \cos\alpha_4} \tag{20}$$

where β_f is the absolute magnitude of the velocity of the receiving station divided by c, and α_4 is the angle between this vector and the line connecting the point of reflection to the point of reception.

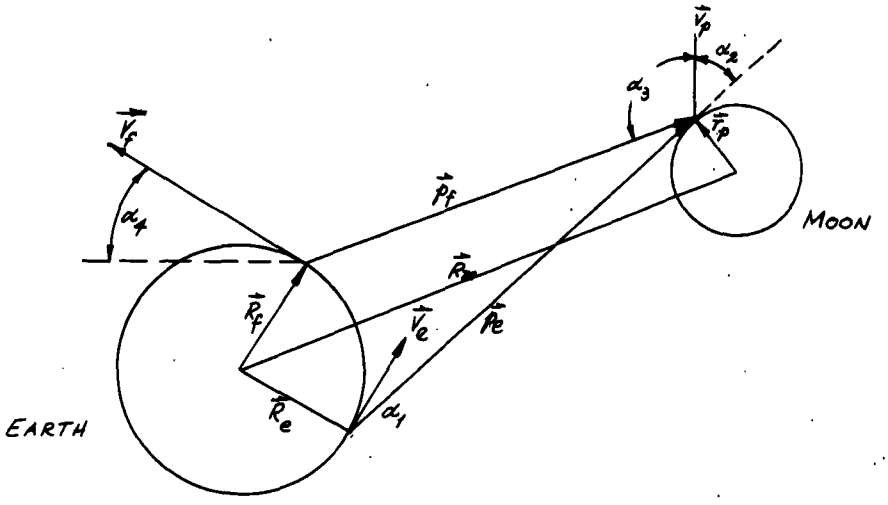

In terms of the vectors illustrated above, the cosines of the relevant transmission angles are as follows:

$$\cos\alpha_1 = \frac{\vec{V}_e \cdot \vec{\rho}_e}{|V_e||\rho_e|} \qquad \cos\alpha_2 = \frac{\vec{V}_p \cdot \vec{\rho}_e}{|V_p||\rho_e|}$$

$$\cos\alpha_3 = \frac{-\vec{V}_p \cdot \vec{\rho}_f}{|V_p||\rho_f|} \qquad \cos\alpha_4 = \frac{-\vec{V}_f \cdot \vec{\rho}_f}{|V_f||\rho_f|} \tag{21}$$

where $\vec{V}_e$ = velocity of the transmission point on earth

$\vec{V}_p$ = velocity of the reflection point on the moon

$\vec{V}_f$ = velocity of the reception point on the earth

$\vec{\rho}_e = \vec{R}_m + \vec{r}_p - \vec{R}_e$

$\vec{\rho}_f = \vec{R}_m + \vec{r}_p - \vec{R}_f$

Combining all the intermediate shifts in observed frequency, the received frequency is found to be

$$\omega_4 = \omega_0 \frac{\sqrt{1-\beta_e^2}}{\sqrt{1-\beta_f^2}} \frac{(1-\beta_f \cos\alpha_4)}{(1-\beta_e \cos\alpha_1)} \frac{(1-\beta_p \cos\alpha_2)}{(1-\beta_p \cos\alpha_3)} \tag{22}$$

5. PLAN OF CALCULATION

From the foregoing discussion it is clear that the received frequency will vary with the moon's position in the sky and the location of the reflection point on the surface of the moon. The reflection point of greatest interest is the point of specular reflection, where the vectors $\vec{\rho}_e$ and $\vec{\rho}_f$ make equal angles with the moon's radius vector $\vec{r}_p$. This point wanders only a few degrees at most from the center of the visible disc, as an examination of the geometry will show.

Since to the incident beam the moon will present surfaces oriented in many directions, in the shape of crater floors, mountain sides, and so forth, it is to be expected that reflection toward Buffalo will not be confined to the specular reflection point. Thus the Doppler shifts in energy received from these other points are of interest, as they will "beat" against the central frequency, causing low-frequency fading in the received signal.